

SHAPING THE GLOBULAR CLUSTER MASS FUNCTION BY STELLAR-DYNAMICAL EVAPORATION

DEAN E. McLAUGHLIN^{1,2} AND S. MICHAEL FALL^{3,4}

The Astrophysical Journal, in press

ABSTRACT

We show that the globular cluster mass function (GCMF) in the Milky Way depends on cluster half-mass density, ρ_h , in the sense that the mass M_{TO} at which the GCMF turns over increases with ρ_h while the width of the distribution decreases. We argue that this behavior is expected if a peak in the GCMF is the result of slow depletion, predominantly through cluster evaporation driven by internal two-body relaxation, of a mass function that originally rose as a power law towards low masses—a process previously shown by Fall & Zhang to explain the shape of the current GCMF below M_{TO} . We fit the full GCMF as a function of ρ_h with models in which the average mass-loss rates of clusters in the past are estimated from their current densities according to $-dM/dt = \mu_{\text{ev}} \propto \rho_h^{1/2}$. We then use the observed ρ_h of individual GCs in bins of Galactocentric radius (r_{gc}) and concentration (c) as input to the same models, to predict GCMF dependences on r_{gc} and c that are in good agreement with observations. Thus, such dependences directly reflect details of the distribution of ρ_h over r_{gc} and c . In particular, we recover the well-known insensitivity of M_{TO} to Galactocentric radius. This feature does not derive from a literal “universality” of the GCMF peak mass, but from a significant variation of M_{TO} with ρ_h , which is expected to result from relaxation-driven cluster disruption, plus significant scatter in ρ_h as a function of r_{gc} .

We show that all of these results still hold if the evaporation rates of clusters are taken to depend on the mean volume densities ρ_t or surface densities Σ_t inside their tidal radii, as $\mu_{\text{ev}} \propto \rho_t^{1/2}$ or $\mu_{\text{ev}} \propto \Sigma_t^{3/4}$ —alternative formulations that are also physically motivated but involve working with cluster properties that are not as well defined or as readily observable, in general, as ρ_h . In any case, the normalization of μ_{ev} required to fit the GCMF implies cluster lifetimes that may be slightly on the short side but are well within range of standard values for relaxation-driven evaporation. The success of models such as these places constraints on the importance of gravitational shocks in shaping a dynamically evolved GCMF, since shock-driven mass-loss rates have an inverse dependence on cluster density. Our analysis does not depend on any theoretical assumptions or empirical information about the velocity-anisotropy profile of the Galactic GC system.

Subject headings: galaxies: star clusters—globular clusters: general

1. INTRODUCTION

The mass functions of star cluster systems provide an important point of reference for attempts to understand the connection between old globular clusters (GCs) and the young massive clusters that form in local starbursts and galaxy mergers. When expressed as the number per unit logarithmic mass, $dN/d \log M$, the GC mass function (GCMF) is characterized by a peak, or turnover, at a mass $M_{\text{TO}} \approx 1\text{--}2 \times 10^5 M_\odot$ that is empirically very similar in most galaxies. By contrast, the mass functions of young clusters show no such feature but instead rise monotonically towards low masses over the full observed range ($10^6 M_\odot \gtrsim M \gtrsim 10^4 M_\odot$ in the best-studied cases), in a way that is well described by a power law, $dN/d \log M \propto M^{1-\beta}$ with $\beta \simeq 2$ (e.g., Zhang & Fall 1999).

At the same time, for high $M > M_{\text{TO}}$, old GCMFs closely resemble the mass functions of young clusters, and of molecular clouds in the Milky Way and other galaxies (Harris & Pudritz 1994; Elmegreen & Efremov 1997); and it is well known that a number of dynamical processes cause star clusters to lose mass and can lead to their complete destruction

as they orbit for a Hubble time in the potential wells of their parent galaxies (e.g., Fall & Rees 1977; Caputo & Castellani 1984; Aguilar, Hut, & Ostriker 1988; Chernoff & Weinberg 1990; Gnedin & Ostriker 1997; Murali & Weinberg 1997). It is therefore natural to ask whether the peaks in GCMFs can be explained by the depletion over many Gyr of globulars from initial mass distributions that were similar to those of young clusters below M_{TO} as well as above.

Our chief purpose in this paper is to establish and interpret an aspect of the Galactic GCMF, which appears fundamental but has gone largely unnoticed to date: $dN/d \log M$ has a strong and systematic dependence on GC half-mass density, $\rho_h \equiv 3M/8\pi r_h^3$ (r_h being the cluster half-mass radius), in the sense that the turnover mass M_{TO} increases and the width of the distribution decreases with increasing ρ_h . As observed facts, these must be explained by any theory of the GCMF. We argue here that they are an expected signature of slow dynamical evolution from a mass function that initially increased towards $M < M_{\text{TO}}$, if the long-term mass loss from surviving GCs has been dominated by stellar escape due to internal, two-body relaxation (which we refer to from now on as either relaxation-driven evaporation or simply evaporation).

Fall & Zhang (2001; hereafter FZ01) explain in detail why cluster evaporation dominates the long-term evolution of the low-mass shape of observable GCMFs. Briefly, stellar evolution removes (through supernovae and winds) the same *fraction* of mass from all clusters of a given age, and so cannot change the shape of $dN/d \log M$ (unless special initial con-

¹ Dept. of Physics and Astronomy, University of Leicester, University Road, Leicester, UK LE1 7RH

² Permanent address: Astrophysics Group, Lennard-Jones Laboratories, Keele University, Keele, Staffordshire, UK ST5 5BG; dem@astro.keele.ac.uk

³ Institute for Advanced Study, Einstein Drive, Princeton, NJ 08450

⁴ Permanent address: Space Telescope Science Institute, 3700 San Martin Drive, Baltimore, MD 21218; fall@stsci.edu

ditions are invoked; cf. Vesperini & Zepf 2003). Meanwhile, for GCs like those that have survived for a Hubble time in the Milky Way, the integrated mass loss from gravitational shocks during disk crossings and bulge passages is generally much less than that due to evaporation (see also Gnedin, Lee, & Ostriker 1999; Prieto & Gnedin 2006).⁵

As we discuss further in §2 below, the evaporation of tidally limited clusters proceeds at a rate, $\mu_{\text{ev}} \equiv -dM/dt$, that is approximately constant in time and primarily determined by cluster density. FZ01 show that a constant mass-loss rate leads to a power-law scaling $dN/d \log M \propto M^{1-\beta}$ with $\beta \rightarrow 0$ (corresponding to a flat distribution of clusters per unit *linear* mass) at sufficiently low $M < \mu_{\text{ev}} t$ in the evolved mass function of coeval GCs that began with *any* nontrivial initial $dN/d \log M_0$.⁶ To accommodate this when $dN/d \log M_0$ originally increased towards low masses as a power law, a time-dependent peak must develop in the GCMF at a mass of order $M_{\text{TO}}(t) \sim \mu_{\text{ev}} t$ (FZ01). But then, since μ_{ev} depends fundamentally on cluster density, so too must M_{TO} .

A $\beta \approx 0$ power-law scaling below the turnover mass has been confirmed directly in the GCMFs of the Milky Way (FZ01) and the giant elliptical M87 (Waters et al. 2006), while Jordán et al. (2007) show it to be consistent with $dN/d \log M$ data for 89 Virgo Cluster galaxies, and it is apparent in deep observations of some other GCMFs (e.g., in the Sombrero galaxy, M104; Spitler et al. 2006). As regards the peak itself, old GCs are observed (e.g., Jordán et al. 2005) to have rather similar densities on average—and, therefore, similar typical μ_{ev} —in galaxies with widely different total luminosities and Hubble types. (Inasmuch as cluster densities are set by tides, this is probably related to the mild variation of mean *galaxy* density with total luminosity; see FZ01, and also Jordán et al. 2007.) Thus, an evaporation-dominated evolutionary origin for a turnover in the GCMF appears to be consistent with the well-known fact that the mass scale M_{TO} generally differs very little among galaxies (e.g., Harris 2001; Jordán et al. 2006).

If this picture is basically correct, it implies that, even though M_{TO} may appear nearly universal when considering the global mass functions of entire GC systems, in fact the GCMFs of subsamples of clusters with similar ages but different densities should have different turnovers. In §2, we show—working for definiteness and relatively easy observability with the half-mass density, ρ_h —that this is the case for globulars in the Milky Way. We fit the observed $dN/d \log M$ for GCs in bins of different ρ_h with models assuming that (1) the initial distribution increased as a $\beta = 2$ power law at low masses and (2) the mass-loss rates of individual clusters can be estimated from their half-mass densities by the rule $\mu_{\text{ev}} \propto \rho_h^{1/2}$. In §3 we discuss the validity of this prescription for μ_{ev} , which is certainly approximate but captures the main physical dependence of relaxation-driven mass loss. In particular, we show that the alternative mass-loss laws $\mu_{\text{ev}} \propto \rho_t^{1/2}$ and $\mu_{\text{ev}} \propto \Sigma_t^{3/4}$ —where ρ_t and Σ_t are the mean volume and surface densities inside cluster tidal radii—lead to models for

the GCMF that are essentially indistinguishable from those based on $\mu_{\text{ev}} \propto \rho_h^{1/2}$. The normalization of μ_{ev} required to fit the observed GCMF implies cluster lifetimes that are within a factor of ≈ 2 (perhaps slightly on the low side, if the initial power-law exponent at low masses was $\beta = 2$) of typical values in theories and simulations of two-body relaxation in tidally limited GCs.

We also show in §2 that when the observed densities of individual clusters are used in our models to predict GCMFs in different bins of Galactocentric radius (r_{gc}), they fit the much weaker variation of $dN/d \log M$ and M_{TO} as functions of r_{gc} , which is well-known in the Milky Way and other large galaxies (see Harris 2001; Harris, Harris, & McLaughlin 1998; Barmby, Huchra, & Brodie 2001; Vesperini et al. 2003; Jordán et al. 2007). Similarly, applying our models to the GCs in two bins of central concentration, with only the measured ρ_h of the clusters in each subsample as input, suffices to account for previously noted differences between the mass functions of low- and high-concentration Galactic globulars (Smith & Burkert 2002). The most fundamental feature of the GCMF therefore appears to be its dependence on cluster density, which can be understood at least qualitatively (and even quantitatively, at the factor-of-two level to which our simple models are realistic) in terms of evaporation-dominated cluster disruption.

There is a widespread perception that if the GCMF evolved slowly from a rising power law at low masses, then a weak or null variation of M_{TO} with r_{gc} can be achieved only in GC systems with strongly radially anisotropic velocity distributions, which are not observed (see especially Vesperini et al. 2003). This apparent inconsistency has been cited to bolster some recent attempts to identify a mechanism by which a “universal” peak at $M_{\text{TO}} \sim 10^5 M_\odot$ might have been imprinted on the GCMF at the time of cluster formation, or very shortly afterwards, and little affected by the subsequent destruction of lower-mass GCs (e.g., Vesperini & Zepf 2003; Parmentier & Gilmore 2007). However, given the real successes of an evaporation-dominated evolutionary scenario for the origin of M_{TO} , as summarized above and added to below, it would be premature to reject the idea in favor of *requiring* a near-formation origin, solely on the basis of difficulties with GC kinematics. (And, in any event, formation-oriented models must now be reconsidered in light of the *non-universality* of M_{TO} as a function of cluster density.)

We are not concerned in this paper with velocity anisotropy in GC systems, because we only predict an evaporation-evolved $dN/d \log M$ as a function of cluster density (and age) and take the observed distribution of ρ_h versus r_{gc} in the Milky Way as a given, to show consistency with the current behavior of M_{TO} as a function of r_{gc} . Most other models (FZ01; Vesperini et al. 2003; and references therein) predict dynamically evolved GCMFs directly in terms of r_{gc} , and in doing so are forced also to derive theoretical dependences of cluster density on r_{gc} . It is only at this stage that GC orbital distributions enter the problem, and then only in conjunction with several other assumptions and simplifications. As we discuss further in §3 below, the radially biased GC velocity distributions that appear in such models could well be artifacts of one or more of these other assumptions, rather than of the main hypothesis about evaporation-dominated GCMF evolution.

⁵ It is possible that there existed a past population of GCs with low densities or concentrations, or perhaps on extreme orbits, that were destroyed in less than a Hubble time by shocks or stellar evolution. Our discussion does not cover such clusters.

⁶ Throughout this paper, we use “initial” to mean at a relatively early time in the development of long-lived clusters, after they have dispersed any remnants of their natal gas clouds, survived the bulk of stellar-evolution mass loss, and come into virial equilibrium in the tidal field of a galaxy.

2. THE GALACTIC GCMF AS A FUNCTION OF CLUSTER DENSITY

In this section we define and model the dependence of the Galactic GCMF on cluster density. First, we describe the dependence that is expected to arise from evaporation-dominated evolution.

Two-body relaxation in a tidally limited GC leads to a roughly steady rate of mass loss, $\mu_{\text{ev}} \equiv -dM/dt \simeq \text{constant}$ in time. Thus, the total cluster mass decreases approximately linearly, as $M(t) \simeq M_0 - \mu_{\text{ev}} t$. This behavior is exact in some classic models of GC evolution (Hénon 1961) and is found to be a good approximation in all other calculations (e.g., Lee & Ostriker 1987; Chernoff & Weinberg 1990; Vesperini & Heggie 1997; Gnedin, Lee, & Ostriker 1999; Baumgardt 2001; Giersz 2001; Baumgardt & Makino 2003; Trenti, Heggie, & Hut 2007). The result comes from a variety of computational methods (semi-analytical, Fokker-Planck, Monte Carlo, and N -body simulation) applied to clusters with different initial conditions (densities and concentrations) on different kinds of orbits (circular and eccentric; with and without external gravitational shocks) and with different internal processes and ingredients (including or ignoring stellar-evolution mass loss and close stellar interactions; with or without stellar mass spectra, binaries, and central black holes). To be sure, deviations from perfect linearity in $M(t)$ do occur, but these are generally small—especially away from the endpoints of the evolution, i.e., for $0.9 \gtrsim M(t)/M_0 \gtrsim 0.1$ —and neglecting them to assume an approximately constant dM/dt is entirely adequate for our purposes.

When gravitational shocks are subdominant to relaxation-driven evaporation, as they generally appear to be for extant GCs, they work to boost the mass-loss rate μ_{ev} slightly without altering the basic linearity of $M(t)$ (e.g., Gnedin, Lee, & Ostriker 1999; see also Figure 1 of FZ01). A time-dependent mass scale $\Delta \equiv \mu_{\text{ev}} t$ is then associated naturally with any system of coeval clusters having a common mass-loss rate: all those with initial $M_0 \leq \Delta$ are disrupted by time t , and replaced with the remnants of objects that began with $M_0 > \Delta$. As we mentioned in §1, if the initial GCMF increased towards low masses as a power law, then Δ is closely related to a peak in the evolved distribution, which eventually decreases towards very low $M(t) < \Delta$ as $dN/d \log M \propto M^{1-\beta}$ with $\beta = 0$ (FZ01).

In standard theory (e.g., Spitzer 1987; Binney & Tremaine 1987, Section 8.3), the lifetime of a cluster against evaporation is a multiple of its two-body relaxation time, t_{rlx} . For a total mass M of stars within a radius r , this scales to first order (ignoring a weak mass dependence in the Coulomb logarithm) as $t_{\text{rlx}}(r) \propto (Mr^3)^{1/2} \propto M/\rho^{1/2}$, where $\rho \propto M/r^3$. In a concentrated cluster with an internal density gradient, $t_{\text{rlx}}(r)$ of course varies throughout the cluster, and the global relaxation timescale is an average of the local values (see the early discussion by King 1958). This can still be written as $t_{\text{rlx}} \propto M/\bar{\rho}^{1/2}$, with M the total cluster mass and $\bar{\rho}$ an appropriate reference density. We then have for the instantaneous mass-loss rate, $\mu_{\text{ev}} \equiv -dM/dt \propto M/t_{\text{rlx}} \propto \bar{\rho}^{1/2}$. Insofar as this is approximately constant in time, a GCMF evolving from an initial $\beta > 1$ power law at low masses should therefore develop a peak at a mass that depends on cluster density and age through the parameter $\Delta \propto \bar{\rho}^{1/2} t$.

It remains to identify the best measure of $\bar{\rho}$ in this context. A standard choice in the literature, and the one that we eventually make to derive our main results in this paper, is the half-mass density $\rho_h = 3M/8\pi r_h^3$. However, in a steady tidal field, the mean density ρ_t inside the tidal radius of a cluster is constant by definition, and thus choosing $\bar{\rho} = \rho_t$ instead is the

simplest way to ensure that $\mu_{\text{ev}} \propto \bar{\rho}^{1/2}$ and $\mu_{\text{ev}} \simeq \text{constant}$ in time are mutually consistent. In fact, King (1966) found from direct calculations of the escape rate at each radius within his standard (lowered Maxwellian) models, that the coefficient in $\mu_{\text{ev}} \propto \rho_t^{1/2}$ is only a weak function of the internal density structure (concentration) of the models, and thus only a weak function of time for a cluster evolving quasistatically through a series of such equilibria.

The rule $\mu_{\text{ev}} \propto \rho_t^{1/2}$ is routinely used to set the GC mass-loss rates in models for the dynamical evolution of the GCMF, although such studies normally express μ_{ev} immediately in terms of orbital pericenters, r_p , most often by assuming $\rho_t \propto r_p^{-2}$ as for GCs in galaxies whose total mass distributions follow a singular isothermal sphere (e.g., Vesperini 1997, 1998, 2000, 2001; Vesperini et al. 2003; Baumgardt 1998; FZ01). This bypasses any explicit examination of the GCMF as a function of cluster density, which is our main goal in this paper. But it is done in part because tidal radii are the most poorly constrained of all structural parameters for GCs in the Milky Way (their theoretical definition is imprecise and their empirical estimation is highly model-dependent and sensitive to low-surface brightness data), and they are exceedingly difficult if not impossible to measure in distant galaxies. We deal with this here by focusing on the GCMF as a function of cluster density ρ_h inside the less ambiguous, empirically better determined and more robust half-mass radius, asking how simple models with $\mu_{\text{ev}} \propto \rho_h^{1/2}$ fare against the data.

Taking $\mu_{\text{ev}} \propto \rho_h^{1/2}$ in place of $\mu_{\text{ev}} \propto \rho_t^{1/2}$, which we do to construct evaporation-evolved model GCMFs in §2.2, is most appropriate if the ratio ρ_t/ρ_h is the same for all clusters and constant in time. This is the case in Hénon’s (1961) model of GC evolution, and in this limit (adopted by FZ01 in their models for the Galactic GCMF) our analysis is rigorously justified. However, real clusters are not homologous (ρ_t/ρ_h differs among clusters) and they do not evolve self-similarly (ρ_h may vary in time even if ρ_t does not). The key assumption in our models is that μ_{ev} is approximately independent of time for any GC, which is well-founded in any case. By using current ρ_h values to estimate μ_{ev} , we do not suppose that the half-mass densities are also constant, but we in effect use a single number for all GCs to represent a range of $(\rho_t/\rho_h)^{1/2}$. Equivalently, we ignore a dependence on cluster concentration in the normalization of $\mu_{\text{ev}} \propto \rho_h^{1/2}$. As we discuss further in §3, it is reasonable to neglect this complication in a first approximation because $(\rho_t/\rho_h)^{1/2}$ varies much less among Galactic globulars than ρ_t and ρ_h do separately. We demonstrate this explicitly by repeating our analysis with ρ_h replaced by ρ_t and recover essentially the same results for the GCMF.

In §3 we also discuss some recent results, which indicate that the timescale for relaxation-driven evaporation depends on a slightly less-than-linear power of t_{rlx} (Baumgardt 2001; Baumgardt & Makino 2003). We point out that this implies that μ_{ev} may increase as a modest power of the average *surface* density of a cluster as well as (or, in an important special case, instead of) the usual volume density. However, we show in detail that making the appropriate changes throughout the rest of the present section to reflect this possibility does not qualitatively change any of our conclusions.

2.1. Data

Figure 1 shows the distribution of mass against half-mass density and against Galactocentric radius for 146 Milky Way

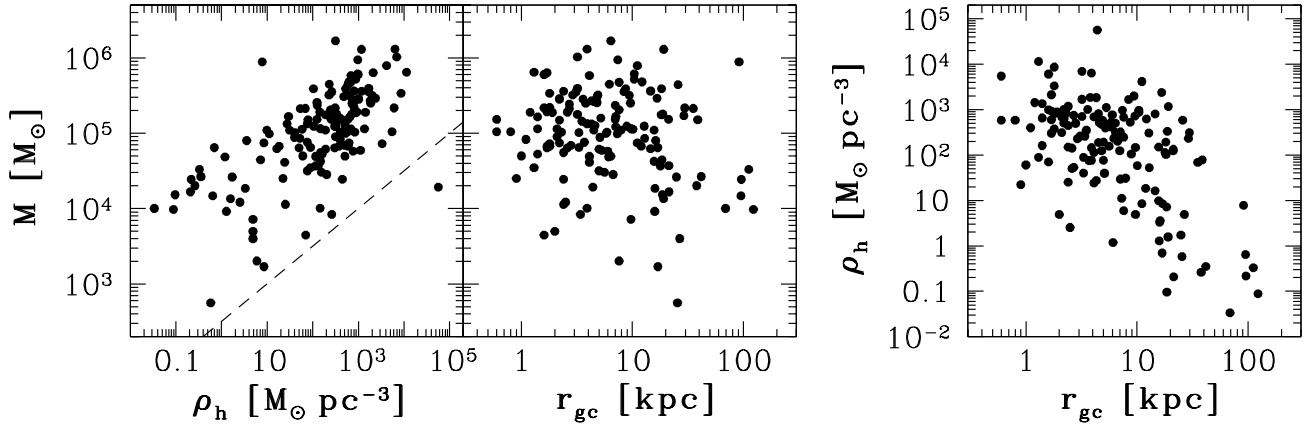


FIG. 1.— *Left*: Mass versus three-dimensional half-mass density, $\rho_h \equiv 3M/8\pi r_h^3$, and versus Galactocentric radius, r_{gc} , for 146 Milky Way GCs in the catalogue of Harris (1996). The dashed line in the first panel is $M \propto \rho_h^{1/2}$, a locus of approximately constant lifetime against evaporation. *Right*: Half-mass density versus r_{gc} for the same clusters.

GCs in the catalogue of Harris (1996),⁷ along with the distribution of ρ_h versus r_{gc} linking the two mass plots. The Harris catalogue actually records the absolute V magnitudes of the GCs. We obtain masses from these by applying the population-synthesis model mass-to-light ratios Υ_V computed by McLaughlin & van der Marel (2005) for individual clusters based on their metallicities and an assumed age of 13 Gyr. However, we first multiplied all of the McLaughlin & van der Marel Υ_V values by a factor of 0.8 so as to obtain a median $\hat{\Upsilon}_V \simeq 1.5 M_\odot L_\odot^{-1}$ in the end,⁸ consistent with direct dynamical estimates (see McLaughlin 2000 and McLaughlin & van der Marel 2005; also Barmby et al. 2007).

By assigning mass-to-light ratios to GCs in this way, we allow for expected differences between clusters with different metallicities. Our application of a corrective factor to the population-synthesis values, Υ_V^{pop} , is motivated empirically by the fact that their distribution among Galactic GCs is strongly peaked around a median $\hat{\Upsilon}_V^{\text{pop}} \simeq 1.9 M_\odot L_\odot^{-1}$, while the observed (dynamical) Υ_V^{dyn} lie in a fairly narrow range around $\hat{\Upsilon}_V^{\text{dyn}} \simeq 1.5 M_\odot L_\odot^{-1}$ (McLaughlin & van der Marel 2005). However, it is worth noting that the size of this discrepancy is similar to what is found in some numerical simulations of two-body relaxation over a Hubble time in clusters with a spectrum of stellar masses (e.g., Baumgardt & Makino 2003). In such simulations, Υ_V^{dyn} falls below Υ_V^{pop} due to the preferential escape of low-mass stars with high individual M_*/L_* (population-synthesis models do not incorporate this or any other stellar-dynamical effect). Thus, a median $\hat{\Upsilon}_V^{\text{dyn}} < \hat{\Upsilon}_V^{\text{pop}}$ may itself be a signature of cluster evaporation. We might then also expect that more dynamically evolved clusters—that is, those with shorter relaxation times—could have systematically lower ratios of $\Upsilon_V^{\text{dyn}}/\Upsilon_V^{\text{pop}}$. However, this is a relatively small effect, which is not well quantified theoretically and is not clearly evident in real data (the numbers published by McLaughlin & van der Marel 2005 show no significant correlation between $\Upsilon_V^{\text{dyn}}/\Upsilon_V^{\text{pop}}$ and t_{th} for Galactic globulars). We therefore proceed, as stated, with a single $\Upsilon_V^{\text{dyn}}/\Upsilon_V^{\text{pop}} = 0.8$ assumed for all GCs.

Harris (1996) gives the projected half-light radius R_h for

141 of the clusters with a mass estimated in this way, and for these we obtain the three-dimensional half-mass radius from the general rule $r_h = (4/3)R_h$ (Spitzer 1987), which assumes no internal mass segregation. The remaining five objects have mass estimates but no size measurements. To each of these clusters, we assign an r_h equal to the median value for those of the first 141 GCs having masses within a factor two of the one with unknown r_h . In all cases, the half-mass density is $\rho_h \equiv 3M/8\pi r_h^3$.

The leftmost panel in Figure 1 shows immediately that the cluster mass distribution has a strong dependence on half-mass density: the median \hat{M} increases with ρ_h while the scatter in $\log M$ —that is, the width of the GCMF—decreases. The first of these points is related to the fact that r_h correlates poorly with M (e.g., Djorgovski & Meylan 1994; McLaughlin 2000). The second point, that the dispersion of $dN/d \log M$ decreases with increasing ρ_h , is behind the finding (Kavelaars & Hanes 1997; Gnedin 1997) that the GCMF is broader at very large Galactocentric radii. We return to this in §2.2.

A natural concern, when plotting M against ρ_h as we have done here, is that any apparent correlation might only be a trivial reflection of the definition $\rho_h \propto M/r_h^3$. This may seem particularly worrisome because, as we just mentioned, it is known that size does not correlate especially well with mass for GCs in the Milky Way (or, indeed, in other galaxies). However, the lack of a tight M – r_h correlation does *not* imply that all GCs have *the same* r_h , even within the unavoidable measurement errors. The root-mean-square (rms) scatter of $\log r_h$ about its average value is ± 0.3 for Galactic GCs, and the 68-percentile spread in $\log r_h$ is slightly greater than 0.5, or more than a factor of 3 in linear terms (from the data in Harris 1996; see, e.g., Figure 8 of McLaughlin 2000). This compares to an rms random measurement error (from formal, χ^2 fitting uncertainties) of $\delta(\log r_h) \approx 0.05$, or about 10% relative error; and an rms systematic measurement error (i.e., differences in the r_h inferred from fitting different structural models to a single cluster) of perhaps $\delta(\log r_h) \lesssim 0.03$; see McLaughlin & van der Marel (2005). Most of the scatter in plots of observed half-light radius versus mass is therefore real and contains physical information. The left-hand panel of Figure 1 displays this information in a form that highlights clear, nontrivial overall trends requiring physical explanation.

The dashed line in the plot of mass against density traces

⁷ Feb. 2003 version; see <http://physwww.mcmaster.ca/~harris/mwgc.dat>.

⁸ Throughout this paper, we use \hat{x} to denote the median of any quantity x .

TABLE 1
MILKY WAY GC PROPERTIES IN BINS OF DENSITY AND GALACTOCENTRIC RADIUS

Bin	\mathcal{N}	$\hat{\rho}_h^a$ [$M_\odot \text{ pc}^{-3}$]	\hat{r}_{gc}^a [kpc]	M_{\min} [M_\odot]	M_{\max} [M_\odot]	\hat{M}^a [M_\odot]	M_{TO}^b [M_\odot]
ρ_h bins							
$0.034 \leq \rho_h \leq 76.5 M_\odot \text{ pc}^{-3}$	48	8.48	12.9	5.63×10^2	8.84×10^5	4.12×10^4	3.98×10^4
$78.8 \leq \rho_h \leq 526 M_\odot \text{ pc}^{-3}$	49	232	5.6	8.37×10^3	1.67×10^6	1.22×10^5	1.58×10^5
$579 \leq \rho_h \leq 5.65 \times 10^4 M_\odot \text{ pc}^{-3}$	49	973	3.2	1.93×10^4	1.30×10^6	2.82×10^5	2.88×10^5
r_{gc} bins							
$0.6 \leq r_{gc} \leq 3.2 \text{ kpc}$	47	597	1.9	4.47×10^3	1.02×10^6	1.15×10^5	2.14×10^5
$3.3 \leq r_{gc} \leq 9.4 \text{ kpc}$	50	261	5.2	2.02×10^3	1.67×10^6	1.27×10^5	1.66×10^5
$9.6 \leq r_{gc} \leq 123 \text{ kpc}$	49	18.4	18.3	5.63×10^2	1.30×10^6	7.42×10^4	8.71×10^4

^aThe notation \hat{x} represents the median of quantity x .

^b M_{TO} is the peak mass of the *model* GCMFs traced by the solid curves in each panel of Figure 2, which are given by equation (3) of the text with $\beta = 2$, $M_c = 10^6 M_\odot$, and individual Δ given by the observed ρ_h of each cluster through equation (4).

the proportionality $M \propto \rho_h^{1/2}$, or $Mr_h^3 = \text{constant}$. Insofar as the half-mass relaxation time scales as $t_{\text{rh}} \propto (Mr_h^3)^{1/2}$, and to the extent that $\mu_{\text{ev}} \propto M/t_{\text{rh}} \propto \rho_h^{1/2}$ approximates the average rate of relaxation-driven mass loss, this line is one of equal evaporation time. That such a locus nicely bounds the lower envelope of the observed cluster distribution is itself a strong hint that relaxation-driven cluster disruption has significantly modified the GCMF at low masses (recall that $Mr_h^3 = \text{constant}$ defines one side of the GC “survival triangle” when the M – ρ_h plot is recast as r_h versus M : Fall & Rees 1977; Okazaki & Tosa 1995; Ostriker & Gnedin 1997; Gnedin & Ostriker 1997). It is also further evidence that the weak correlation of observed r_h with M is due to significant and real differences in cluster radii, since if r_h were intrinsically the same for all GCs, then we would see $M \propto \rho_h$ instead.

The middle panel of Figure 1 shows the well-known result that the typical GC mass depends weakly if at all on Galactocentric radius, at least until large $r_{gc} \gtrsim 30$ –40 kpc, where there are too few clusters to discern any trend. The right-hand panel of the figure shows why this is true even though the GCMF depends significantly on cluster density: although there is a correlation between half-mass density and Galactocentric position, the large scatter about it is such that convolving the observed M versus ρ_h with the observed ρ_h versus r_{gc} results in an almost null dependence of M on r_{gc} .

We now divide the GC sample in Figure 1 roughly into thirds, in two different ways: first on the basis of half-mass density, and second by Galactocentric radius. These ρ_h and r_{gc} bins are defined in Table 1, which also gives a few summary statistics for the globulars in each subsample. We count the clusters in every subsample in about 10 equal-width bins of $\log M$ to obtain histogram representations of $dN/d \log M$, first as a function of ρ_h and then as a function of r_{gc} . These GCMFs are shown by the points in Figure 2, with errorbars indicating standard Poisson uncertainties. The curves in the figure trace model GCMFs, which we describe in §2.2. For the moment, it is important to note that the dashed curve is the same in every panel, apart from minor differences in normalization, and is proportional to the GCMF for the whole sample of 146 GCs. (In the middle-left panel of Figure 2, which pertains to clusters distributed tightly around the median ρ_h of the entire GC system, the dashed curve is coincident with the

solid curve running through the data.)

The left-hand panels of Figure 2 show directly that the GCMF is peaked for clusters at any density, and that the mass of the peak increases systematically with ρ_h (see also the last column of Table 1, but note that the turnover masses there refer to the *model* GCMFs that we develop below). The statistical significance of this is very high, and qualitatively it is the behavior expected if M_{TO} owes its existence to cluster disruption at a rate that increases with ρ_h , as is the case with relaxation-driven evaporation.

The right-hand panels of Figure 2 confirm once again that the GCMF peak mass is a very weak function of Galactocentric position. In fact, the observed distributions in the two r_{gc} bins inside $\simeq 10$ kpc are statistically indistinguishable in their entirety, and the main difference at larger $r_{gc} \gtrsim 10$ kpc is a slightly higher proportion of low-mass clusters rather than a large change in M_{TO} . All of this is consistent with the primary dependence of the GCMF being that on ρ_h , since Figure 1 shows that the GC density distribution is not sensitive to Galactocentric position for $r_{gc} \lesssim 10$ –20 kpc but has a substantial low-density tail at larger radii (with a broader associated GCMF, as seen in the upper-left panel of Figure 2).

2.2. Simple Models

We now attempt to assess more quantitatively whether these results are consistent with evaporation-dominated evolution of the GCMF from an initial distribution like that observed for young clusters in the local universe. We model the time-evolution of the distribution of M versus ρ_h in Figure 1 but do not attempt this for the distribution of ρ_h over r_{gc} —the details of which likely depend on a complicated interplay between the tidal field of the Galaxy, the present and past orbital parameters of clusters, and the structural nonhomology of GCs. To compare our models to the current GCMF as a function of r_{gc} , we simply calculate them using the observed ρ_h of individual clusters in different ranges of Galactocentric radius.

We assume that the initial GCMF was independent of cluster density, and that any globulars surviving to the present day have been losing mass for the past Hubble time at constant rates. We use the *current* half-mass density of each cluster to *estimate* $\mu_{\text{ev}} \propto \rho_h^{1/2}$. As we discussed earlier, an approximately time-independent μ_{ev} is indicated by virtually all calculations of two-body relaxation in tidally limited GCs. We

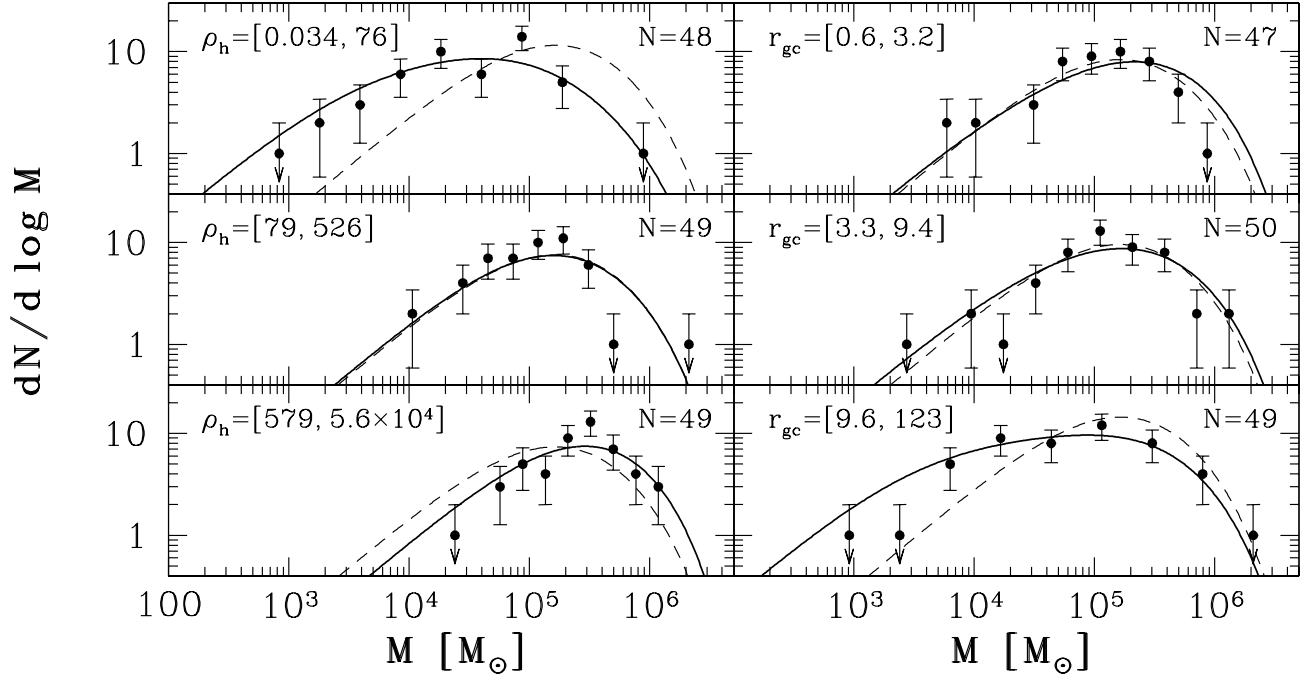


FIG. 2.— GCMF as a function of half-mass density, $\rho_h \equiv 3M/8\pi r_h^3$ (left panels), and as a function of Galactocentric radius, r_{gc} (right panels), for 146 Milky Way GCs in the catalogue of Harris (1996). The dashed curve in all cases is an evolved Schechter function for the entire GC system (Jordán et al. 2007): equation (3) with $\beta = 2$, $M_c = 10^6 M_\odot$, and $\Delta \equiv 2.3 \times 10^5 M_\odot$ for all clusters (from equation [4] and a median $\hat{\rho}_h = 246 M_\odot \text{pc}^{-3}$), giving a peak at $M_{TO} = 1.6 \times 10^5 M_\odot$. Solid curves are the GCMFs predicted by equation (3) with $\beta = 2$ and $M_c = 10^6 M_\odot$ but individual Δ given by the observed ρ_h of each cluster (equation [4]) in the different subsamples.

give a more detailed, a posteriori justification in §3 for using ρ_h , rather than other plausible measures of cluster density, to estimate μ_{ev} .

Consider first a group of coeval GCs with an initial mass function $dN/d \log M_0$ and a single, time-independent mass-loss rate μ_{ev} . The mass of every cluster decreases linearly as $M(t) = M_0 - \mu_{ev}t$, and at any later time each has lost the same amount $\Delta \equiv M_0 - M(t) = \mu_{ev}t$. FZ01 show rigorously that in this case, the evolved and initial GCMFs are related by

$$\frac{dN}{d \log M} = \frac{M}{M_0} \times \frac{dN}{d \log M_0} = \frac{M}{(M + \Delta)} \frac{dN}{d \log (M + \Delta)}. \quad (1)$$

This is the basis for the claim that the mass function scales generically as $dN/d \log M \propto M^{\beta+1}$ ($\beta = 0$ power law) at low enough $M(t) < \Delta$ —that is, for the surviving remnants of clusters with $M_0 \approx \Delta$ —just so long as the initial distribution was not a delta function.

We follow FZ01 (see also Jordán et al. 2007) in adopting a Schechter (1976) function for the initial GCMF:

$$dN/d \log M_0 \propto M_0^{1-\beta} \exp(-M_0/M_c). \quad (2)$$

With $\beta \simeq 2$, this distribution describes the power-law mass functions of young massive clusters in systems like the Antennae galaxies (e.g., Zhang & Fall 1999). An exponential cut-off at $M_c \sim 10^6 M_\odot$ is generally consistent with such data, even if not always demanded by them; here we require it mainly to match the curvature observed at high masses in old GCMFs (e.g., Burkert & Smith 2000; Jordán et al. 2007).

Combining equations (1) and (2) gives the probability density that a single GC with known evaporation rate and age has an instantaneous mass M . The time-dependent GCMF of a system of \mathcal{N} GCs with a range of μ_{ev} (or ages, or both) is

then just the sum of all such individual probability densities:

$$\frac{dN}{d \log M} = \sum_{i=1}^{\mathcal{N}} \frac{A_i M}{[M + \Delta_i]^\beta} \exp\left[-\frac{M + \Delta_i}{M_c}\right]. \quad (3)$$

Here the total mass losses $\Delta_i = (\mu_{ev}t)_i$ may differ from cluster to cluster (t_i being the age of a single GC) but both β and M_c are assumed to be constants, independent of ρ_h in particular.⁹ Given each Δ_i , the normalizations A_i in equation (3) are defined so that the integral over $d \log M$ of each term in the summation is unity.

Jordán et al. (2007) have introduced a specialization of equation (3) in which all clusters have the same Δ . They refer to this as an evolved Schechter function and describe its properties in detail (including giving a formula for the turnover mass M_{TO} as a function of Δ and M_c) for the case $\beta = 2$. Here we note only that, at very young cluster ages or for slow mass-loss rates, such that $\Delta \ll M_c$ and only the low-mass, power-law part of the initial GCMF is significantly eroded, any one evolved Schechter function has a peak at $M_{TO} \simeq \Delta/(\beta - 1)$ (for $\beta > 1$). As Δ increases relative to M_c , the turnover at first increases proportionately and the width of the distribution decreases (since the high-mass end at $M \gtrsim M_{TO}$ is largely unchanged). For large $\Delta \gg M_c$, however, the peak is bounded above by $M_{TO} \rightarrow M_c$ and the width approaches a lower limit.¹⁰

⁹ Note that M_c appears to take on different values in the GCMFs of other galaxies, varying systematically with the total luminosity L_{gal} (Jordán et al. 2007). The reasons for this are unclear, as is the origin of this mass scale in the first place.

¹⁰ The increase of M_{TO} and the decrease of the full width of $dN/d \log M$ for increasing Δ eventually saturate when the mass loss per GC is so high that it affects clusters in the exponential part of the initial Schechter-function GCMF. This is because $dN/d \log M \propto M^{\beta+1} \exp(-M/M_c)$ is a self-similar solution to the evolution equation (1).

Thus, the dependence of M_{TO} on Δ is weaker than linear when M_c is finite in the initial GCMF of equation (2). Any peak in the full equation (3) for a system of GCs with individual Δ values is an average of \mathcal{N} different turnovers and must be calculated numerically.

In their modeling of the Milky Way GC system, FZ01 effectively compute mass functions of the type (3)—based on the same initial conditions and dynamical evolution—with a distribution of Δ values determined by the orbital parameters of clusters in an idealized, spherical and static logarithmic Galaxy potential (used both to fix μ_{ev} in terms of cluster tidal densities and to estimate additional mass loss due to gravitational shocks). Jordán et al. (2007) fit GCMF data in the Milky Way and scores of Virgo Cluster galaxies with their version of equation (3) in which all GCs have the same Δ . They thus estimate the dynamical mass loss from *typical* clusters in these systems. Here, we construct models for the Milky Way GCMF using Δ values given directly by the observed half-mass densities of individual GCs.

We adopt $\beta = 2$ for the initial low-mass power-law index in equation (2), which carries over into equation (3) for the evolved $dN/d \log M$. Jordán et al. (2007) have fitted the full Galactic GCMF with an evolved Schechter function assuming $\beta = 2$ and a single $\Delta \equiv \hat{\Delta}$ for all surviving globulars. They find $M_c \simeq 10^6 M_\odot$ and $\hat{\Delta} = 2.3 \times 10^5 M_\odot$. We use this value of M_c in equation (3) and we associate $\hat{\Delta}$ with the mass loss from clusters at the median half-mass density of the entire GC system, which is $\hat{\rho}_h = 246 M_\odot \text{pc}^{-3}$ from the data in Figure 1. Since we are assuming that $\Delta = \mu_{\text{ev}} t \propto \rho_h^{1/2} t$ for coeval GCs, we therefore stipulate

$$\Delta = 1.45 \times 10^4 M_\odot (\rho_h / M_\odot \text{pc}^{-3})^{1/2} \quad (4)$$

for globulars with arbitrary ρ_h . Assuming a typical GC age of $t = 13$ Gyr, this corresponds to a mass-loss rate of

$$\mu_{\text{ev}} \simeq 1100 M_\odot \text{Gyr}^{-1} (\rho_h / M_\odot \text{pc}^{-3})^{1/2}. \quad (5)$$

In §3 we discuss the cluster lifetimes implied by this value of μ_{ev} . We emphasize here that the scaling of μ_{ev} and Δ with $\rho_h^{1/2}$ follows rather generically from our hypothesis of evaporation-dominated cluster evolution, while the numerical coefficients in equations (4) and (5) are specific to the assumption of $\beta = 2$ for the power-law index at low masses in the initial GCMF.

The dashed curve shown in every panel of Figure 2 is the evolved Schechter function fitted to the entire GCMF of the Milky Way by Jordán et al. (2007). This has a peak at $M_{\text{TO}} \simeq 1.6 \times 10^5 M_\odot$ (magnitude $M_V \simeq -7.4$ for a typical V-band mass-to-light ratio of 1.5 in solar units) and gives a very good description of the observed $dN/d \log M$ in the middle density bin, $79 \lesssim \rho_h \lesssim 530 M_\odot \text{pc}^{-3}$, and in the two inner radius bins, $r_{\text{gc}} \leq 9.4$ kpc. This is expected, since the median half-mass density in each of these cluster subsamples is very close to the system-wide median $\hat{\rho}_h = 246 M_\odot \text{pc}^{-3}$ (see Table 1). Even in the outermost r_{gc} bin, a Kolmogorov-Smirnov (KS) test only marginally rejects the dashed-line model (at the $\simeq 95\%$ level), because this subsample still includes many GCs at or near the global median $\hat{\rho}_h$ (see Figure 1). By contrast, the average GCMF is strongly rejected as a model for the lowest- and highest-density GCs on the left-hand side of Figure 2: the KS probabilities that these data are drawn from the dashed distribution are $< 10^{-4}$ in both cases. This is also expected since, by construction, these bins only contain clusters with densities well away from the median of the full GC

system, for which the total mass lost to evaporation should be significantly different from the typical $\hat{\Delta} = \Delta(\hat{\rho}_h)$.

The solid curves in Figure 2, which are different in every panel, are the superpositions of many different evolved Schechter functions, as in equation (3), with distinct Δ values given by equation (4) using the observed ρ_h of each cluster in the corresponding subsample. These models provide excellent matches to the observed $dN/d \log M$ in every ρ_h and r_{gc} bin, with $\chi^2 < 1.3$ per degree of freedom in all cases. This is the main result of this paper.

The last column of Table 1 gives the mass M_{TO} at which each of the solid *model* GCMFs in Figure 2 peaks. We note that these turnovers increase roughly as $M_{\text{TO}} \sim \hat{\rho}_h^{0.3-0.4}$ for our specific binnings in ρ_h and r_{gc} , somewhat shallower than the $\rho_h^{1/2}$ scaling of the cluster mass-loss rate that defines the models. This is partly because of the averaging over many individual turnovers implied by the summation of several evolved Schechter functions in each GC bin, and partly because—as we discussed just after equation (3)—the turnover mass of any one evolved Schechter function cannot increase indefinitely in direct proportion to $\Delta \propto \rho_h^{1/2}$, but has a strict upper limit of $M_{\text{TO}} \leq M_c$.

Our models are naturally consistent with the fact that the GCMF is narrower for clusters with higher densities. This is obvious in the left-hand panels of Figure 2; in the discussion immediately after equation (3), we described how it follows from the increase of M_{TO} with $\Delta \propto \rho_h^{1/2}$ for a single evolved Schechter function. In addition, the superposition of many such functions with separate, density-dependent turnovers and widths results in wider GCMFs for cluster subsamples spanning larger ranges of ρ_h . This accounts in particular for the breadth of the mass function at $r_{\text{gc}} \geq 9.4$ kpc. The globulars at these radii have $0.034 \leq \rho_h \leq 4.1 \times 10^3 M_\odot \text{pc}^{-3}$, corresponding to individual evolved Schechter functions with turnovers at $2.7 \times 10^3 \lesssim M_{\text{TO}} \lesssim 4.0 \times 10^5 M_\odot$. The composite GCMF in the lower-right panel of Figure 2 therefore extremely broad and shows a very flat peak, such that an overall M_{TO} cannot be established precisely from the data alone. This explains the findings of Kavelaars & Hanes (1997), who pointed out that the GCMF of the outermost third of the Milky Way cluster system has a turnover that is statistically consistent with the full-Galaxy average, but a larger dispersion (see also Gnedin 1997).

Finally, if the GCMF evolved dynamically from initial conditions similar to those we have adopted, then the data and models in the left-hand panels of Figure 2 argue against the notion that external gravitational shocks, rather than internal two-body relaxation, might have mainly driven the evolution of the present GC population. This is because, while evaporation-dominated cluster disruption involves mass-loss rates that increase as a positive power of GC density, shocks alone lead to rates that are *inversely* proportional to density: $\mu_{\text{sh}} \propto M/\rho_h$, with a constant of proportionality that depends on details of the GC orbit (i.e., the frequency of disk crossings or bulge passages) and the internal structure of the cluster. Thus, with the GC system split into ρ_h bins as in Figure 2, shock-dominated evolution would be expected to result in the GCMF for the highest-density globulars being *less* evolved, and closer in form to the initial $dN/d \log M_0$, than that for the lowest-density clusters—the opposite of what is observed. (We note, however, that gravitational shocks may have been important in destroying very massive or very low-

density clusters early in the history of our Galaxy.)

2.3. Other Cluster Properties

If the current shape of the GCMF is fundamentally the result of long-term cluster disruption according to a mass-loss rule like $\mu_{\text{ev}} \propto \rho_h^{1/2}$, then it should be possible to reproduce the distribution as a function of any other cluster attribute by using the observed ρ_h of individual GCs in equations (3) and (4) to build model $dN/d \log M$ for subsamples of the Galactic cluster system defined by any criteria—as we did for the r_{gc} binning of §2.2. Here we explore one example in which differences in the GCMFs of two groups of globulars can be seen in this way to follow from differences in their ρ_h distributions.

Smith & Burkert (2002) have shown that the mass function of Galactic globulars with King (1966) model concentrations $c < 0.99$ has a less massive peak than that for $c \geq 0.99$. [Here $c \equiv \log(r_t/r_0)$, where r_t is the fitted tidal radius and r_0 a core scale.] They further find that a power-law fit to the low- c GCMF just below its peak returns $dN/d \log M \propto M^{+0.5}$ —shallower than the M^{+1} expected generically for a mass-loss rate that is constant in time—but they confirm that the latter slope applies for the GCMF at $c \geq 0.99$. They discuss various options to explain these results, including a suggestion that, if the mass functions of both low- and high-concentration clusters evolved slowly from the same, young-cluster-like initial distribution, then the mass-loss law for low- c GCs may have differed from that for high- c clusters. However, they give no physical explanation for such a difference, and we can show now that none is required.

The upper panel of Figure 3 plots concentration against half-mass density for the same 146 GCs from Figure 1; the filled circles distinguish 24 clusters with $c < 0.99$. There is a correlation of sorts between c and ρ_h , which either derives from or causes the better-known correlation between c and M (e.g., Djorgovski & Meylan 1994; McLaughlin 2000). The important point here is that the ρ_h distribution is offset to lower values and has a higher dispersion at $c < 0.99$. Following the discussion in §2.2, we therefore *expect* the low-concentration GCMF to have a smaller M_{TO} , a flatter shape around the peak, and a larger full width than the high-concentration GCMF.

The lower panel of Figure 3 shows the GCMFs for $c < 0.99$ (filled circles) and $c \geq 0.99$ (open circles). The curves are again given by equation (3) with $\beta = 2$, $M_c = 10^6 M_\odot$, and individual Δ related to the observed ρ_h through equation (4). These models peak at $M_{\text{TO}} \simeq 4.3 \times 10^4 M_\odot$ for the $c < 0.99$ subsample but at $M_{\text{TO}} \simeq 1.8 \times 10^5 M_\odot$ for $c \geq 0.99$, entirely as a result of the different ρ_h involved. The larger width of $dN/d \log M$ and its shallower slope at any $M \lesssim 10^5 M_\odot$ for the low-concentration GCs are also clear, in the model curves as well as the data. It is further evident that there are no low- c Galactic globulars observed with $M \gtrsim 2 \times 10^5 M_\odot$, above the nominal turnover of the full GCMF (as Smith & Burkert 2002 noted). But this is not surprising, given that there are so few low-concentration clusters in total and they are expected to be dominated by low-mass objects because of their generally low densities. Thus, the solid curve in Figure 3 predicts perhaps $\simeq 3$ high-mass clusters with $c < 0.99$, where none is found.

The apparent variation of the Milky Way GCMF with internal concentration is therefore consistent with the same density-based model for evaporation-dominated dynamical evolution that we compared to $dN/d \log M$ as a function of ρ_h and r_{gc} in §2.2. To show this, we have made use of the

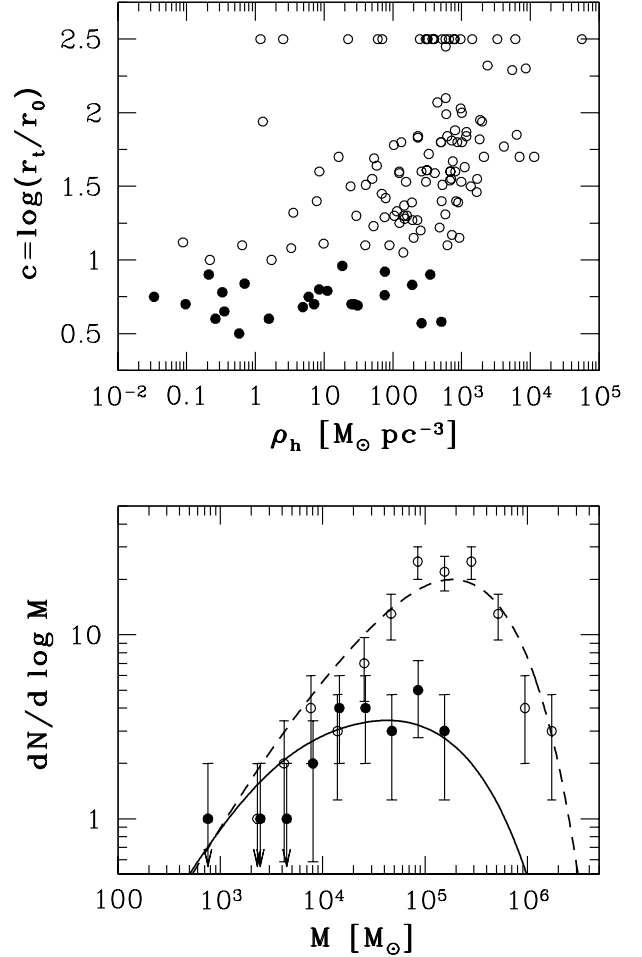


FIG. 3.— *Top*: Concentration parameter as a function of half-mass density for 146 Galactic GCs. The line of points at $c \equiv 2.5$ comes from the practice of assigning this value to core-collapsed clusters in the Harris (1996) catalogue and its sources. *Bottom*: GCMF data and models (eqs. [3] and [4]) for 24 clusters with $c < 0.99$ (filled circles and solid curve) and 122 clusters with $c \geq 0.99$ (open circles and dashed curve).

densities ρ_h exactly as observed within the two concentration bins indicated in Figure 3—just as we also took ρ_h directly from the data for GCs in different ranges of r_{gc} to construct models for comparison with the observed $dN/d \log M$ in the right-hand panels of Figure 2. Of course, this is not the same as *explaining* the distribution of ρ_h versus r_{gc} or c . Doing so would certainly be of interest in its own right, but it is beyond the scope of our work here.

3. DISCUSSION

In this section, we first show that the mass-loss rate in equation (5) above implies total cluster lifetimes that compare favorably with those expected from relaxation-driven evaporation. Then we discuss why it is reasonable to approximate $\mu_{\text{ev}} \propto \rho_h^{1/2}$ in the first place. Finally, we address the issue of possible conflict, in some other models for evaporation-dominated GCMF evolution, between the near-constancy of M_{TO} as a function of r_{gc} and the observed kinematics of GC systems.

3.1. Cluster Lifetimes

The disruption time of a GC with mass M and a steady mass-loss rate μ_{ev} is just $t_{\text{dis}} = M/\mu_{\text{ev}}$. It is convenient,

for purposes of comparison with evaporation times in the literature, to normalize t_{dis} to the relaxation time of a cluster at its half-mass radius. In general, this is $t_{\text{rh}} = 0.138 M^{1/2} r_h^{3/2} / [G^{1/2} m_* \ln(\gamma M/m_*)]$, where m_* is the mean stellar mass. For clusters of stars with a single mass, $m_* \simeq 0.7 M_\odot$ and $\gamma \simeq 0.4$ are appropriate (Spitzer 1987; Binney & Tremaine 1987, equation [8-72]), in which case equation (5) for μ_{ev} from our GCMF modeling implies

$$\frac{t_{\text{dis}}}{t_{\text{rh}}} = \frac{M}{\mu_{\text{ev}} t_{\text{rh}}} \simeq 10 \left[\frac{\ln(0.57 M/M_\odot)}{\ln(0.57 \times 10^5)} \right]. \quad (6)$$

Clusters with realistic stellar mass spectra will have slightly different values of m_* and a smaller γ in the calculation of the relaxation time (Giersz & Heggie 1996), which changes the numerical value of $t_{\text{dis}}/t_{\text{rh}}$ somewhat but does not alter any scalings.

We obtained the normalization of $\mu_{\text{ev}} \propto \rho_h^{1/2}$ in §2.2 by fitting to observed GCMFs defined after applying a specific mass-to-light ratio Υ_V to every cluster, with models assuming a specific form for the initial $dN/d \log M_0$. Thus, the result in equation (6) depends both on the median $\hat{\Upsilon}_V$ and on the power-law index β at low masses in the original Schechter-function GCMF. The net scaling, for either single- or multiple-mass clusters, is

$$t_{\text{dis}}/t_{\text{rh}} \propto \hat{\Upsilon}_V^{-1/2} (\beta - 1)^{-1}. \quad (7)$$

To see the dependence of this dimensionless lifetime on $\hat{\Upsilon}_V$, note that we require $\mu_{\text{ev}} \propto \Delta \propto \Upsilon_V$ to fit the mass losses of clusters with a given distribution of luminosities (the direct observables), whereas M/t_{rh} is proportional to $\rho_h^{1/2} \propto \Upsilon_V^{1/2} (L/r_h^3)^{1/2}$. Therefore, $t_{\text{dis}}/t_{\text{rh}} \propto (M/t_{\text{rh}})/\mu_{\text{ev}} \propto \Upsilon_V^{-1/2}$. The mass-to-light ratios adopted in this paper, with a median value of $\hat{\Upsilon}_V \simeq 1.5 M_\odot L_\odot^{-1}$, are tied directly to dynamical determinations (§2.1).

To understand the dependence on β in equation (7), recall first that the coefficients in our expressions for Δ and μ_{ev} as functions of ρ_h (eqs. [4] and [5]) followed from choosing $\beta = 2$ for the power-law exponent at low masses in the initial GCMF (equation [2]). As we mentioned just after equation (3), the turnover mass of an evolved Schechter function with any $\beta > 1$ is $M_{\text{TO}} \simeq \Delta/(\beta - 1)$ in the limit of low $\Delta \propto \rho_h^{1/2}$, and $M_{\text{TO}} \rightarrow M_c$ for very high Δ . In this sense, the strongest observational constraints on the normalizations of Δ and μ_{ev} come from the low-density clusters. All other things being equal, their GCMF can be reproduced with $\beta \neq 2$ if Δ and μ_{ev} are multiplied by $(\beta - 1)$ at fixed ρ_h . Therefore, $t_{\text{dis}} \propto 1/\mu_{\text{ev}} \propto 1/(\beta - 1)$. Observations of young massive clusters (e.g., Zhang & Fall 1999) suggest that β is near 2; but if it were slightly shallower, then the cluster lifetimes we infer from the old GCMF would increase accordingly. Even a relatively minor change to $\beta = 1.5$ would double $t_{\text{dis}}/t_{\text{rh}}$ from ≈ 10 to ≈ 20 .

In the model of Hénon (1961) for single-mass clusters evolving self-similarly (fixed ratio ρ_t/ρ_h of mean densities inside the tidal and half-mass radii) in a steady tidal field (ρ_t constant in time), a cluster loses 4.5% of its remaining mass every half-mass relaxation time. The time to complete disruption is therefore $t_{\text{dis}}/t_{\text{rh}} = 1/0.045 \simeq 22$. For non-homologous clusters in a steady tidal field, $t_{\text{dis}}/t_{\text{rh}}$ is a function of central concentration and can differ from the Hénon value by factors of about two. From one-dimensional Fokker-Planck calculations, Gnedin & Ostriker (1997) find $t_{\text{dis}}/t_{\text{rh}} \simeq 10\text{--}40$ for King

(1966) model clusters with c values similar to those found in real GCs. Thus, even though the evaporation time in equation (6) may be slightly shorter than is typically found in theoretical calculations, it is certainly within the range of such calculations. Moreover, the assumptions of a steady tidal field and a single stellar mass in Hénon (1961) and Gnedin & Ostriker (1997) are important. Part of the difference between the typical lifetimes in these particular theoretical treatments and our estimate of $t_{\text{dis}}/t_{\text{rh}}$ from the GCMF is that the former do not include gravitational shocks, which may have accelerated somewhat the evolution of real clusters (although we stress again that shocks do not appear in general to have dominated the evolution of extant Galactic GCs and are not expected to affect the basic time-independence of the net mass-loss rate; see Gnedin, Lee, & Ostriker 1999, FZ01, and Prieto & Gnedin 2006). A spectrum of stellar masses in the clusters may also have contributed to an increase in evaporation rate over the single-mass values (e.g., Johnstone 1993; Lee & Goodman 1995).

Estimates of evaporation times from other numerical methods and for models of multimass clusters can be rather sensitive to the detailed computational techniques and input assumptions and approximations, and differences at roughly the factor-of-two level in $t_{\text{dis}}/t_{\text{rh}}$ between different analyses are not uncommon; see, e.g., Vesperini & Heggie (1997), Takahashi & Portegies Zwart (1998, 2000), Baumgardt (2001), Joshi, Nave, & Rasio (2001), Giersz (2001), and Baumgardt & Makino (2003). Thus, although the lifetimes in these studies tend to be broadly comparable to those in Hénon (1961) and Gnedin & Ostriker (1997), noticeably shorter values do occur in some models. In any case, we are encouraged by consistency to within factors of two or three between estimates of t_{dis} or μ_{ev} by such vastly different methods—one purely observational, based on the mass functions of cluster systems; the other purely theoretical, based on idealized models for the evolution of single clusters—particularly since each method involves several uncertain inputs and parameters.

3.2. Approximating $\mu_{\text{ev}} \propto \rho_h^{1/2}$

3.2.1. Half-mass versus Tidal Density

The dimensionless disruption time in equation (6) is independent of any cluster property other than the Coulomb logarithm because we have used GC half-mass densities to estimate $t_{\text{dis}} = M/\mu_{\text{ev}} \propto M/\rho_h^{1/2}$, while t_{rh} also scales as $M/\rho_h^{1/2}$. However, as we mentioned above, the Fokker-Planck calculations of Gnedin & Ostriker (1997) in particular show that $t_{\text{dis}}/t_{\text{rh}}$ is actually a function of central concentration, c , for King (1966) model clusters in steady tidal fields. The constant of proportionality in $\mu_{\text{ev}} \propto \rho_h^{1/2}$ should therefore also depend on c , a detail that we have neglected to this point. We show now that this has not biased any of our analysis or affected our conclusions.

The dotted curve in Figure 4 illustrates the dependence of $t_{\text{dis}}/t_{\text{rh}}$ on c for single-mass King models, as given by equation (30) of Gnedin & Ostriker (1997). The solid curve is proportional to $(\rho_h/\rho_t)^{1/2} = (r_t^3/2r_h^3)^{1/2}$, which we have calculated as a function of c for these models and multiplied by a constant to compare directly with $t_{\text{dis}}/t_{\text{rh}}$. Evidently, there is an approximate equality $t_{\text{dis}}/t_{\text{rh}} \approx 2.15(\rho_h/\rho_t)^{1/2}$, which holds to within $< 15\%$ over the range of concentrations shown in Figure 4 (note that all but 6 Galactic GCs have $0.7 \leq c \leq 2.5$, corresponding to central potentials $3 \lesssim W_0 \lesssim 11$). Thus, if the

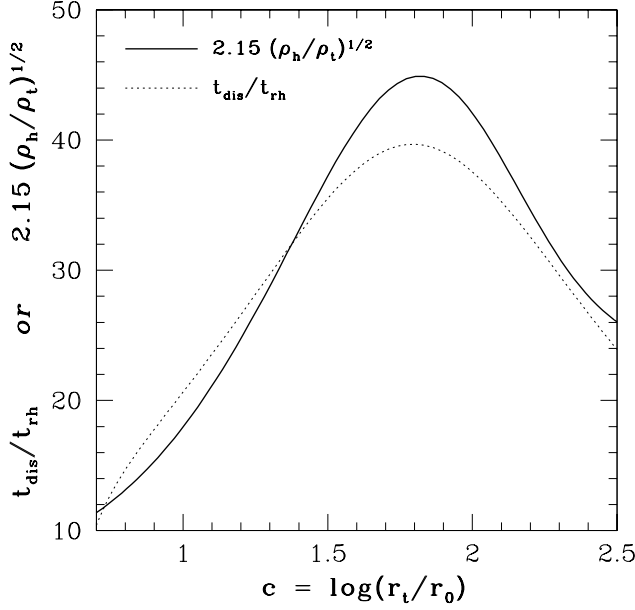


FIG. 4.— Dependence of $t_{\text{dis}}/t_{\text{rh}}$ (dotted line; from Gnedin & Ostriker 1997) and $(\rho_h/\rho_t)^{1/2}$ (solid line; after scaling by a factor of 2.15) on central concentration for single-mass King-model clusters. Over the range of c shown, which includes nearly all Galactic globulars, the approximate proportionality $t_{\text{dis}}/t_{\text{rh}} \propto (\rho_h/\rho_t)^{1/2}$ holds to within better than 15%. Thus, to this level of accuracy the evaporation time t_{dis} is roughly the same multiple of $M/\rho_t^{1/2}$ for clusters with any internal density profile.

evaporation time is written as $t_{\text{dis}} \propto t_{\text{rh}}(\rho_h/\rho_t)^{1/2} \propto M/\rho_t^{1/2}$, then the constant of proportionality in the mass-loss rate $\mu_{\text{ev}} \propto M/t_{\text{dis}} \propto \rho_t^{1/2}$ should be nearly independent of c . In fact, King (1966) originally concluded, from quite basic arguments, that the evaporation rate of a cluster with a lowered-Maxwellian velocity distribution would take the form $\mu_{\text{ev}} \propto \rho_t^{1/2}$ with only a weak dependence on c . An essentially concentration-independent scaling of μ_{ev} with $\rho_t^{1/2}$ is also found in N -body simulations of tidally limited, multimass clusters (e.g., Vesperini & Heggie 1997) and so is not an artifact of any assumptions specific to the calculations of either King (1966) or Gnedin & Ostriker (1997).

This suggests that it might have been more natural to specify cluster evaporation rates proportional to $\rho_t^{1/2}$ rather than $\rho_h^{1/2}$ when developing our GCMF models in §2. For any cluster in a steady tidal field, with a constant ρ_t , such a choice would also have been automatically consistent with an approximately time-independent μ_{ev} and the approximately linear $M(t)$ dependence that we have adopted throughout this paper. As we discussed at the beginning of §2, our decision to work with ρ_h rather than ρ_t was motivated by the fact that the half-mass density is much better defined in principle and more accurately observed in practice. Nevertheless, re-writing $\mu_{\text{ev}} \propto \rho_t^{1/2}$ as $\mu_{\text{ev}} \propto (\rho_t/\rho_h)^{1/2} \times \rho_h^{1/2}$ makes it clear that the validity of our models, with a fixed coefficient in $\mu_{\text{ev}} \propto \rho_h^{1/2}$, depends on the extent to which variations in $(\rho_t/\rho_h)^{1/2}$ can safely be ignored.

Figure 4 shows that the full range of possible values for $(\rho_h/\rho_t)^{1/2}$ in King-model clusters with $c \geq 0.7$ is only a factor of $\simeq 4$ between minimum and maximum. Therefore, using a single, intermediate value of this density ratio to describe all GCs (or a single GC evolving in time through a series of

quasi-static King models)—which we have effectively done by using a GCMF fit to normalize Δ and μ_{ev} in equations (4) and (5)—should never be in error by more than a factor of 2 or so. This is a relatively small inaccuracy, given that measured GC densities range over four to five orders of magnitude.

To confirm more directly that our models with $\mu_{\text{ev}} \propto \rho_h^{1/2}$ are good approximations to GCMF evolution under a mass-loss law $\mu_{\text{ev}} \propto \rho_t^{1/2}$, we have repeated the analysis of §2 in full but using the GC tidal densities ρ_t (derived from the values of r_t listed by Harris 1996) in place of ρ_h throughout. All of our main results persist.

For example, the two panels of Figure 5, which are analogous to the left- and rightmost panels of Figure 1 above, show that (1) the GC mass distribution has a clear dependence on ρ_t , with a lower envelope that is well matched by a line of constant evaporation time, $M \propto \rho_t^{1/2}$ (the dashed line in the plot); and (2) although the scatter in the distribution of ρ_t over Galactocentric radius is smaller than the scatter in ρ_h versus r_{gc} , it is still significant. Because the M - r_{gc} distribution can now be viewed as the convolution of the M - ρ_t distribution with the ρ_t - r_{gc} distribution, the scatter in ρ_t versus r_{gc} is again critical in explaining the weak or null dependence of the GCMF on Galactocentric radius. (The M - r_{gc} distribution is, of course, unchanged from that shown in the middle panel of Figure 1.)¹¹

Figure 6 shows the Milky Way GCMF for globulars in three equally populated bins of tidal density (defined as indicated in the left-hand panels of the plot) and in the same three bins of Galactocentric radius that we used in §2.2 above. Our models for these distributions are based as before on equation (3) with $\beta = 2$, but now the total mass lost from any GC is estimated from its tidal density rather than its half-mass density. Specifically, we take

$$\Delta = 2.1 \times 10^5 M_{\odot} (\rho_t/M_{\odot} \text{pc}^{-3})^{1/2}. \quad (8)$$

The numerical coefficient in equation (8) is such that it gives a Δ identical to that in equation (4) for a GC with $\rho_h/\rho_t = 210$, which is the median value of this density ratio for the 146 GCs in the Harris (1996) catalogue.

As in Figure 2, the dashed curve in every panel of Figure 6 is the same, representing a fit to the average $dN/d \log M$ of the entire Galactic GC system. Thus, it is immediately clear that the peak mass of the GCMF increases significantly and systematically with increasing ρ_t , just as it does with increasing ρ_h . Meanwhile, the solid curves are subsample-specific model GCMFs, obtained by using the observed tidal density of each cluster in any ρ_t or r_{gc} bin to specify individual Δ values via equation (8) for each of the evolved Schechter functions in the summation of equation (3). As expected, there is no appreciable difference, in terms of the fits to any of the observed GCMFs, between these models based on evaporation rates $\mu_{\text{ev}} \propto \rho_t^{1/2}$ and our original models with $\mu_{\text{ev}} \propto \rho_h^{1/2}$.

3.2.2. Retarded Evaporation

Another potential concern comes from recent arguments (see especially Baumgardt 2001; Baumgardt & Makino 2003)

¹¹ As was also the case with our earlier plots involving ρ_h in Figure 1, the scatter and structure in both panels of Figure 5 are real, since the rms scatter of $\log r_t$ about the best-fit lines to either of $\log M$ or $\log r_{\text{gc}}$ is 0.3–0.35 while the rms errorbars based on formal fitting uncertainties are in the range $\delta(\log r_t) \simeq 0.05$ –0.15 for a variety of models (McLaughlin & van der Marel 2005).

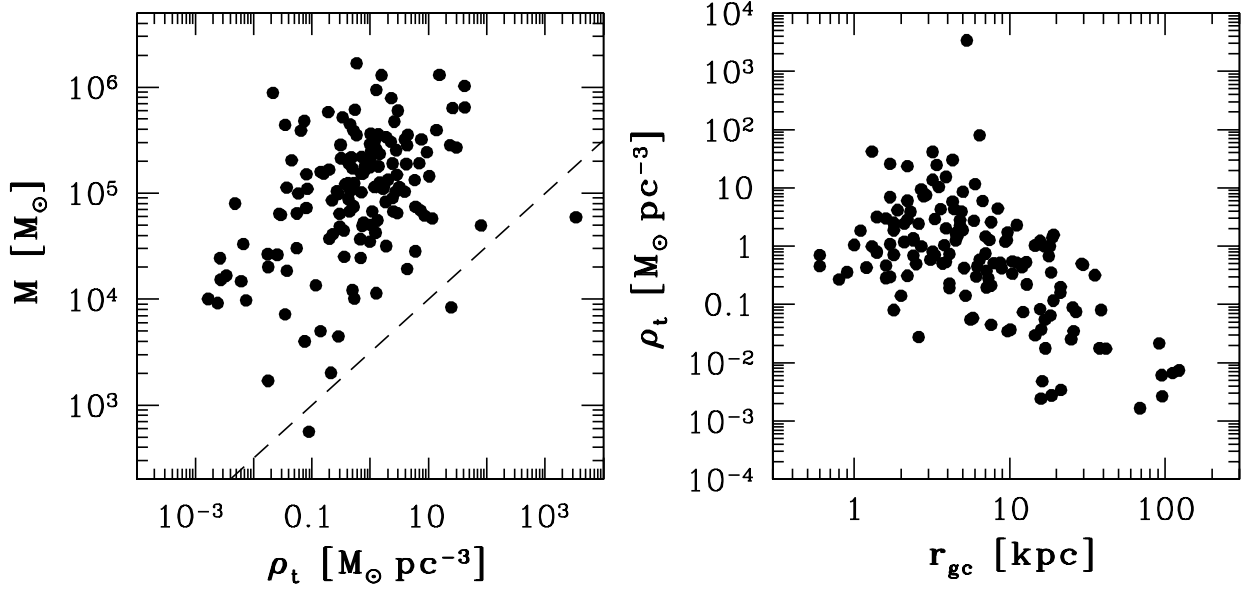


FIG. 5.— Scatter plots of mass M versus mean density inside the tidal radius ($\rho_t \equiv 3M/4\pi r_t^3$) and of ρ_t versus Galactocentric radius r_{gc} , for 146 Galactic GCs from the Harris (1996) catalogue. These plots are analogous to the left- and rightmost panels of Figure 1. The dashed line in the left-hand plot traces the relation $M \propto \rho_t^{1/2}$, a locus of constant evaporation time for $\mu_{ev} \propto \rho_t^{1/2}$.

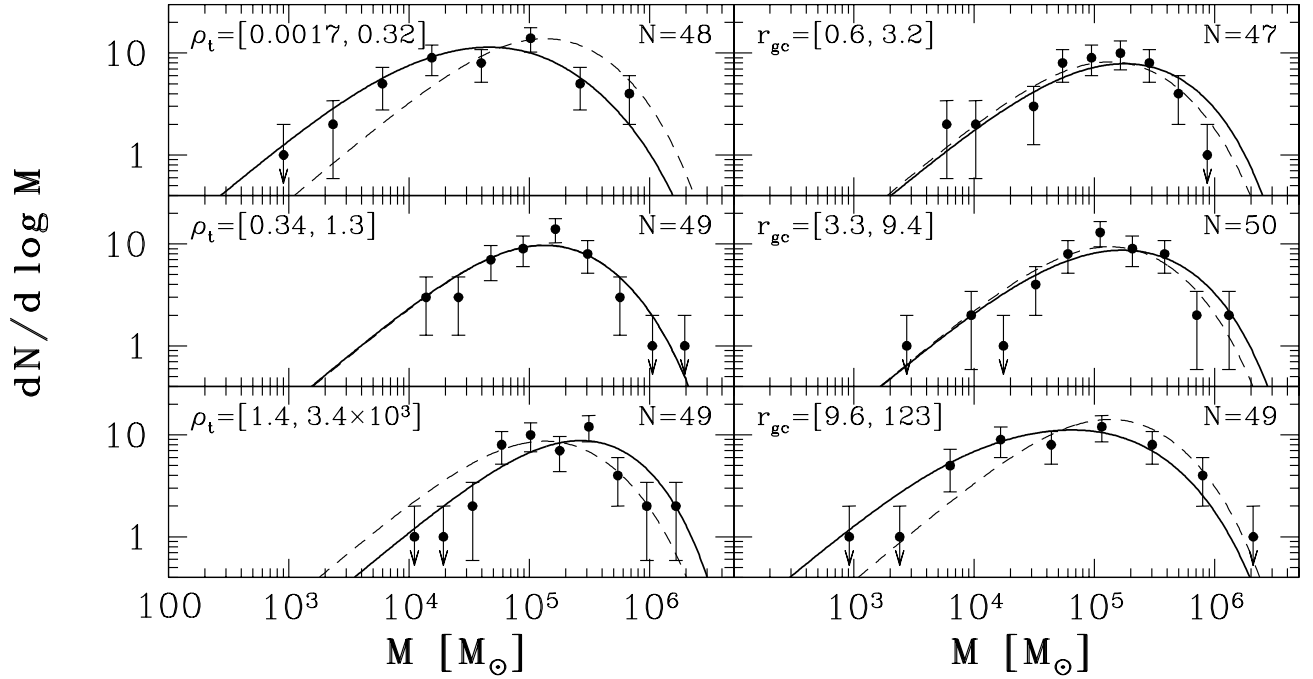


FIG. 6.— Observed GCMF (points, with Poisson errorbars) and models (curves) as a function of mean cluster density inside the tidal radius, $\rho_t \equiv 3M/4\pi r_t^3$ (left-hand panels), and as a function of Galactocentric radius, r_{gc} (right-hand panels). The dashed curve in every panel is an evolved Schechter function representing the entire GC system: equation (3) with $\beta = 2$, $M_c = 10^6 M_\odot$, and a single Δ , common to all clusters, evaluated from equation (8) using the median $\hat{\rho}_t$ of all 146 Galactic GCs. Solid curves are subsample-specific models using equation (3) with $\beta = 2$ and $M_c = 10^6 M_\odot$ but a different Δ value for every cluster (obtained from equation [8] using individual observational estimates of ρ_t in any ρ_t or r_{gc} bin).

that the total evaporation time of a tidally limited cluster is not simply a multiple of an internal two-body relaxation time, $t_{rlx} \propto (Mr^3)^{1/2}$, but depends on both t_{rlx} and the crossing time $t_{cr} \propto (M/r^3)^{-1/2}$ through the combination $t_{dis} \propto t_{rlx}^x t_{cr}^{1-x}$, with $x < 1$. The mass-loss rate $\mu_{ev} \propto M/t_{dis}$ then scales as $M^{3/2-x} r^{-3/2}$, which for $x \neq 1$ differs from the rates $\mu_{ev} \propto \rho_h^{1/2}$ and $\mu_{ev} \propto \rho_t^{1/2}$ that we have so far adopted. However, our

GCMF models are still meaningful, because postulating $t_{dis} \propto t_{rlx}^x t_{cr}^{1-x}$ implies a dependence of μ_{ev} on a measure of cluster density that is, once again, accurately *approximated* by $\rho_h^{1/2}$ for Galactic GCs. Before showing this, we briefly discuss the reasons and the evidence for a possible dependence of t_{dis} on both t_{rlx} and t_{cr} .

If stars are assumed to escape a cluster as soon as they have

attained energies above some critical value as a result of two-body relaxation, then $t_{\text{dis}} \propto t_{\text{rlx}}$ is expected (and confirmed by N -body simulations; e.g., Baumgardt 2001). However, more complicated behavior may arise when escape not only depends on stars satisfying such an energy criterion, but also requires them to cross a spatial boundary. Then, although the stars are still scattered to near- and above-escape energies on the timescale t_{rlx} , they require some additional time to actually leave the cluster. This escape timescale is related fundamentally to t_{cr} (but also depends on details of the stellar orbits, the external tidal field, and the shape of the zero-energy surface). The longer this extra time, the higher is the probability that further encounters with bound cluster stars may scatter any potential escapers back down to sub-escape energies. The net result is a slow-down (“retardation”) of the overall evaporation rate (Chandrasekhar 1942; King 1959; Takahashi & Portegies Zwart 1998, 2000; Fukushima & Heggie 2000; Baumgardt 2001) and a lengthening of the cluster lifetime t_{dis} , by a factor that can be expected to increase with the ratio $t_{\text{cr}}/t_{\text{rlx}}$. If this factor scales as $(t_{\text{cr}}/t_{\text{rlx}})^{1-x}$ for some $x < 1$, then $t_{\text{dis}} \propto t_{\text{rlx}} (t_{\text{cr}}/t_{\text{rlx}})^{1-x} = t_{\text{rlx}}^x t_{\text{cr}}^{1-x}$.

While such a retardation of evaporation can be expected to occur at some level in all clusters, there are physical subtleties in the effect that are probably not captured adequately by a simple re-parametrization of lifetimes as $t_{\text{dis}} \propto t_{\text{rlx}}^x t_{\text{cr}}^{1-x}$. In particular, it is unlikely that this expression can hold for clusters of all masses with a single value of $x < 1$. Since $t_{\text{cr}}/t_{\text{rlx}} \propto M^{-1}$, very massive clusters have $t_{\text{cr}} \ll t_{\text{rlx}}$, and stars scattered to greater than escape energies by relaxation cross the tidal boundary effectively instantaneously—implying that the standard $t_{\text{dis}} \propto t_{\text{rlx}}$, or $x \rightarrow 1$, applies in the high-mass limit. Indeed, if this were not the case, and a fixed $x < 1$ held for all M , then an unphysical $t_{\text{dis}} < t_{\text{rlx}}$ would obtain at high enough masses; see Baumgardt (2001) for further discussion. Unfortunately, “very massive” is not well quantified in this context, and it is not yet clear if a single value of x is accurate for the entire GC mass regime. So far, it has been checked directly only for initial cluster masses below the current peak of the GCMF.

It is also worth noting that the analysis and simulations aimed at this problem to date have dealt with clusters on circular or moderately eccentric orbits in galactic potentials that are static and spherical. This means that any tidal perturbations felt by stars within the clusters are relatively weak and/or slow compared to their own orbital periods, leading to nearly adiabatic or at least non-impulsive responses. In more realistic situations, the galactic potential would be time-dependent and non-spherical and there might be additional tidal perturbations, including disk and bulge shocks. These perturbations could in some cases *accelerate* the escape of weakly bound stars from the clusters and thus counteract the retardation effect to some degree. Further study is therefore needed to determine the regime of validity of the formula $t_{\text{dis}} \propto t_{\text{rlx}}^x t_{\text{cr}}^{1-x}$ and its possible modification outside this regime.

In the meantime, Baumgardt (2001) and Baumgardt & Makino (2003; hereafter BM03) have fitted this formula to the lifetimes of a suite of N -body clusters with initial masses $M_0 \lesssim 7 \times 10^4 M_\odot$ and several different initial concentrations and orbital eccentricities. BM03 at first write t_{dis} in terms of the relaxation and crossing times of clusters at their half-mass radii, so that $t_{\text{rlx}} \propto (Mr_h^3)^{1/2}$, $t_{\text{cr}} \propto (M/r_h^3)^{-1/2}$, and $t_{\text{dis}} \propto M^{x-1/2} r_h^{3/2}$ (see their equation [5]). However, they immediately take a factor of $(r_i/r_h)^{3/2}$ out from the normalization of

this scaling—in effect to obtain $t_{\text{dis}} \propto M^{x-1/2} r_i^{3/2}$ with a different constant of proportionality—and then use a simple definition of the tidal radius (their equation [1], $r_t^3 = GM r_p^2 / 2V_c^2$, which is appropriate for a circular orbit of radius r_p in a logarithmic potential with circular speed V_c ; see Innanen, Harris, & Webbink 1983) to obtain the total lifetime of a cluster as a function of its initial mass, perigalactic distance, and V_c (their equation [7]). A single exponent $x \simeq 0.75$ and a single normalization in this function then suffice to predict to within 10% the lifetimes of the N -body clusters on circular orbits in BM03, regardless of their initial concentrations. By implication, if t_{rlx} and t_{cr} were fixed at r_h rather than r_i , then t_{dis} *would* have an additional concentration dependence, related to the ratio $(r_i/r_h)^{3/2}$ —very similar to what we discussed in §3.2.1 for the case $x = 1$.

We now re-examine the Milky Way GCMF in terms of this prescription for retarded evaporation (bearing in mind the caveats mentioned above). To avoid any explicit dependences on concentration, we also focus on the tidal radius and write $t_{\text{dis}} \propto M^{x-1/2} r_t^{3/2}$ for general $x \leq 1$; but we do not substitute a potential- and orbit-specific formula for r_t in terms of r_p and galactic properties such as V_c . Instead, to keep the emphasis entirely on cluster densities, we re-write the scaling of the lifetime in terms of the mean *surface* density inside the tidal radius, $\Sigma_t \equiv M/\pi r_t^2$, and the corresponding volume density $\rho_t = 3M/4\pi r_t^3$. This leads to $t_{\text{dis}} \propto M \Sigma_t^{-3(1-x)} \rho_t^{-2(x-3/4)}$, which then implies

$$\mu_{\text{ev}} \equiv -dM/dt \propto M/t_{\text{dis}} \propto \Sigma_t^{3(1-x)} \rho_t^{2(x-3/4)}. \quad (9)$$

Clearly, the standard $\mu_{\text{ev}} \propto \rho_t^{1/2}$, which we have already discussed, is recovered for $x = 1$; while for $x = 0.75$, we have the equally straightforward $\mu_{\text{ev}} \propto \Sigma_t^{3/4}$.

BM03 find that, even with the retarded evaporation implied by $x \simeq 0.75$, the masses of their simulated clusters still decrease approximately linearly with time after stellar-evolution effects (which are only important for the first few $\times 10^8$ yr) are separated out; see especially their Figure 6, equation (12), and related discussion. Thus, if the GCMF initially rose towards low masses and has been eroded by slow, relaxation-driven cluster destruction, then in this modified description of evaporation we might expect the current mass function to depend fundamentally on Σ_t rather than ρ_h or ρ_t . But because $M(t)$ still decreases nearly linearly with t , only now with $\mu_{\text{ev}} \propto \Sigma_t^{3/4}$ for each cluster, the shape of the evolved GCMF and its dependence on Σ_t should resemble our earlier results for ρ_h and ρ_t .

We have confirmed this expectation by repeating all of our analyses in §2 again, now using $\mu_{\text{ev}} \propto \Sigma_t^{3/4}$ to estimate cluster mass-loss rates. As before, we calculate Σ_t from the data in the Harris (1996) catalogue, although we caution once more that the catalogued tidal radii, and thus the derived Σ_t , are more uncertain than r_h and ρ_h .

Figure 7, which should be compared to Figures 1 and 5 above, shows that the average Galactic GC mass increases systematically with Σ_t ; that the lower envelope of the M – Σ_t distribution is described well by $M \propto \Sigma_t^{3/4}$ (the dashed line in the left-hand panel of Figure 7), which is a locus of constant lifetime against evaporation for $\mu_{\text{ev}} \propto \Sigma_t^{3/4}$; and that the scatter in the distribution of cluster Σ_t versus Galactocentric radius (right-hand panel of the figure) is substantial, as required to account for the almost non-existent correlation between M and r_{gc} .

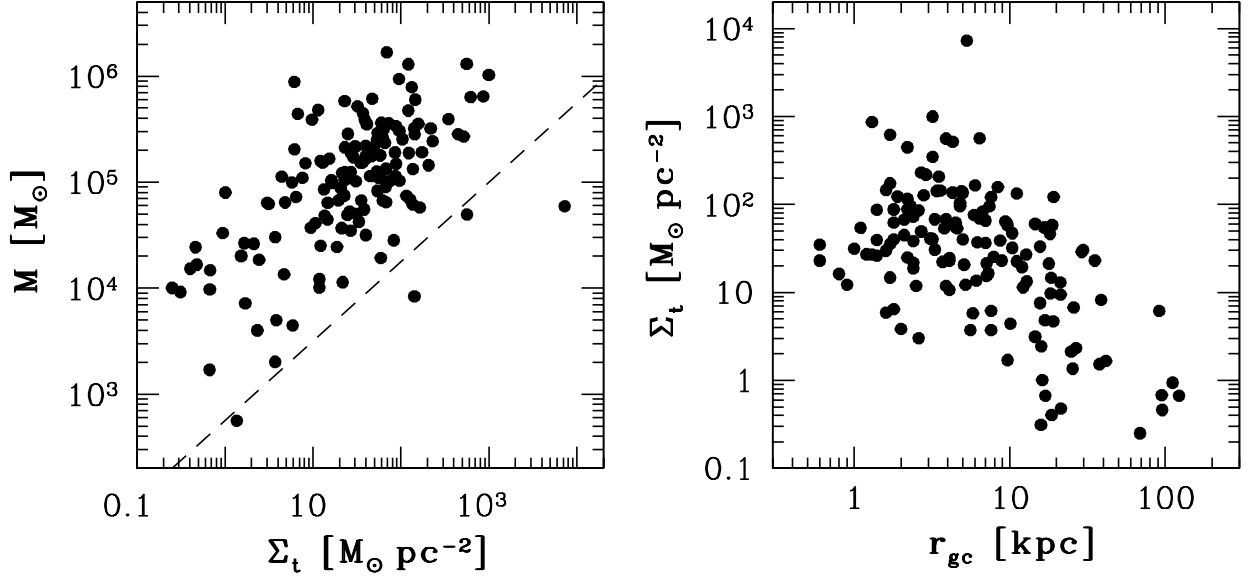


FIG. 7.— Scatter plots of mass M versus mean *surface density* inside the tidal radius ($\Sigma_t \equiv M/\pi r_t^2$) and of Σ_t versus Galactocentric radius r_{gc} , for 146 Galactic GCs from the Harris (1996) catalogue. These plots are analogous to the left- and rightmost panels of Figure 1, and the two panels of Figure 5. The dashed line in the left-hand plot traces the relation $M \propto \Sigma_t^{3/4}$, a locus of constant evaporation time for $\mu_{ev} \propto \Sigma_t^{3/4}$.

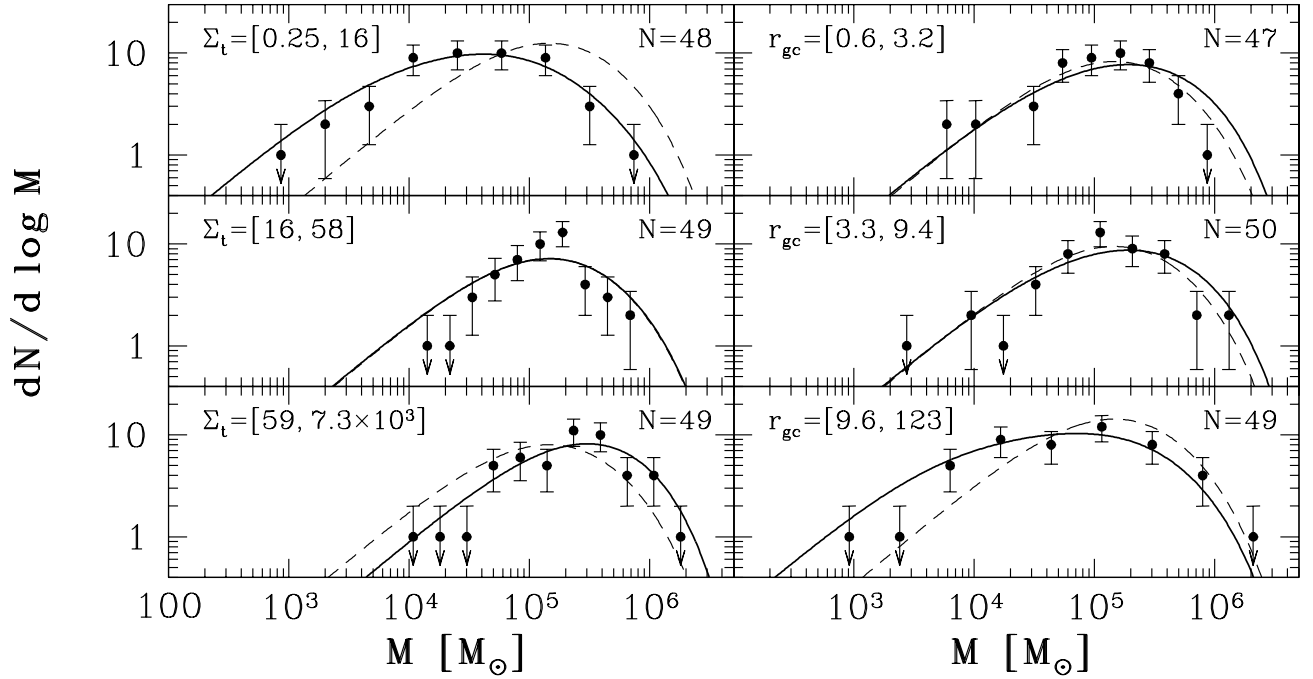


FIG. 8.— Observed GCMF (points, with Poisson errorbars) and models (curves) as a function of mean *surface density* inside the tidal radius, $\Sigma_t \equiv M/\pi r_t^2$ (left-hand panels), and as a function of Galactocentric radius, r_{gc} (right-hand panels). The dashed curve in every panel is an evolved Schechter function representing the entire GC system: equation (3) with $\beta = 2$, $M_c = 10^6 M_\odot$, and a single Δ , common to all clusters, evaluated from equation (10) using the median $\hat{\Sigma}_t$ of all 146 Galactic GCs. Solid curves are subsample-specific models using equation (3) with $\beta = 2$ and $M_c = 10^6 M_\odot$ but a different Δ value for every cluster (obtained from equation [10] using individual observational estimates of Σ_t in any Σ_t or r_{gc} bin).

The left-hand side of Figure 8 shows the mass functions of globulars in three bins of Σ_t , as defined in each panel. The right-hand side of the figure shows $dN/d \log M$ in the same three intervals of r_{gc} as in Figures 2 and 6 above. As in those earlier plots, the dashed curve in all panels of Figure 8 is a model GCMF with the same parameters in every case, representing the mass function of the entire Galactic GC sys-

tem. Once again, compared to the average M_{TO} , the observed turnover mass is significantly lower for clusters in the lowest Σ_t bin and higher for clusters in the highest Σ_t bin, while the width of $dN/d \log M$ decreases noticeably as Σ_t increases.

The solid curves in Figure 8 are again different in every panel. They are the sums of evaporation-evolved Schechter functions as in equation (3), with the usual $\beta = 2$ assumed but

with total mass losses estimated individually for each GC in any Σ_t or r_{gc} bin according to $\Delta \propto \Sigma_t^{3/4}$ rather than $\mu_{ev} \propto \rho_h^{1/2}$ or $\mu_{ev} \propto \rho_t^{1/2}$. However, it turns out not to be necessary to change the *normalization* of $\mu_{ev} \propto \rho_h^{1/2}$ in equation (4) to achieve good fits to the observed GCMF as a function of either Σ_t or r_{gc} . Thus, in Figure 8 we have simply used

$$\Delta = 1.45 \times 10^4 M_\odot (\Sigma_t / M_\odot \text{pc}^{-2})^{3/4}. \quad (10)$$

The fits of these models, based on $t_{dis} \propto t_{rlx}^x t_{cr}^{1-x}$ with $x \simeq 0.75$, are indistinguishable from the fits of our original models based on the standard $t_{dis} \propto t_{rlx}$, i.e., $x = 1$. (We have confirmed that adopting individual Δ given by equation [10] also reproduces the GCMFs of low- and high-concentration GCs in Figure 3 as well as before.) It was perhaps somewhat unexpected that equation (10) and equation (4) should have the same numerical coefficient, but we note that this follows empirically from the fact that the measured ρ_h and Σ_t of Galactic GCs are consistent with the simple near-equality, $\rho_h / M_\odot \text{pc}^{-3} \approx (\Sigma_t / M_\odot \text{pc}^{-2})^{1.5}$ in the mean. This is illustrated in Figure 9, which also shows that there is significant scatter about the relation.¹² However, this scatter does not correlate with cluster mass or Galactocentric radius. From a pragmatic point of view, therefore, $\rho_h^{1/2}$ and $\Sigma_t^{3/4}$ are near enough to interchangeable for our purposes, and there is no practical difference between GCMF models based on one or the other measure of GC density.

One further check on this is to verify that the mass-loss rate associated with equation (10) is roughly in keeping with that implied by the N -body simulations pointing to $x = 0.75$ in the first place. Thus, we compare the rate

$$\mu_{ev} = \Delta / (13 \text{ Gyr}) \simeq 1100 M_\odot \text{Gyr}^{-1} (\Sigma_t / M_\odot \text{pc}^{-2})^{3/4} \quad (11)$$

to a formula implicit in BM03. Starting with their equation (7) for the total lifetime t_{dis} as a function of initial cluster mass and perigalactic distance and circular speed in a logarithmic halo potential; using their $x = 0.75$ and their normalization of 1.91×10^6 yr, multiplied as in their equation (9) by $(1+e)$ to allow for eccentric orbits with apo- and perigalactic distances related by $e \equiv (r_a - r_p) / (r_a + r_p)$; putting in their equation (1) for r_t ; taking the mean mass of cluster stars to be $m_* = 0.55 M_\odot$, as they do; using $\gamma = 0.02$ as they do in the Coulomb logarithm, $\ln(\gamma M_0 / m_*)$; and defining $\Sigma_{t,0} \equiv M_0 / \pi r_{t,0}^2$ (the subscript 0 denoting initial values), we obtain

$$\begin{aligned} \mu_{ev}(\text{BM03}) &\simeq \frac{0.7 M_0}{t_{dis}} \simeq \frac{560}{1+e} M_\odot \text{Gyr}^{-1} \\ &\times \left[\frac{\ln(0.036 M_0 / M_\odot)}{\ln(0.036 \times 10^5)} \right]^{3/4} \left(\frac{\Sigma_{t,0}}{M_\odot \text{pc}^{-2}} \right)^{3/4}. \end{aligned} \quad (12)$$

This is appropriate for clusters that just fill their Roche lobes at perigalacticon, which is where $\Sigma_{t,0}$ is specified. The factor of 0.7 in the first equality accounts for mass loss due to stellar evolution in the BM03 simulations, which, as they discuss,

¹² Although it may be only a coincidence that the constant of proportionality in $\rho_h \propto \Sigma_t^{1.5}$ is so near unity, the basic scaling itself holds because combining the observed correlation between cluster mass and central concentration (Djorgovski & Meylan 1994; McLaughlin 2000) with the intrinsic dependence of r_t / r_h on c in King models leads roughly to $(r_t / r_h) \propto M^{1/6}$.

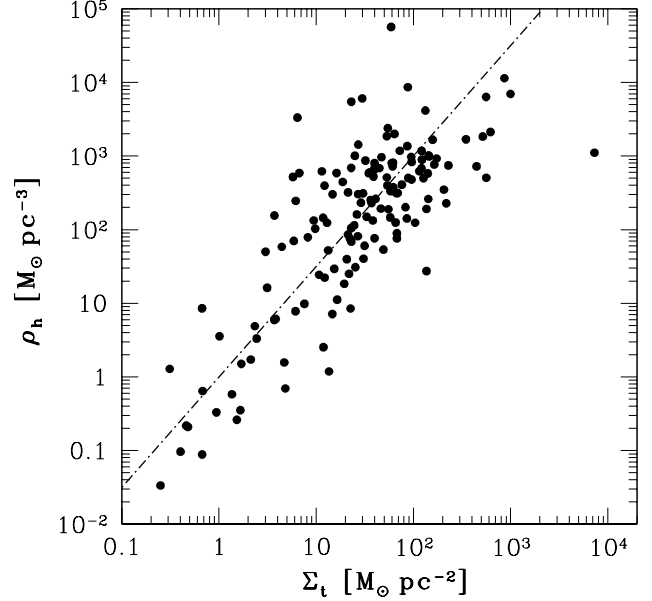


FIG. 9.— Half-mass density, $\rho_h = 3M/8\pi r_h^3$, against mean surface density inside the tidal radius, $\Sigma_t = M/\pi r_t^2$, for 146 clusters with data in Harris (1996). The straight line is $\rho_h = \Sigma_t^{1.5}$.

can be treated as having occurred almost immediately and in full at the beginning of a cluster's life.

Our GCMF-based μ_{ev} is a factor of ≈ 2 faster than the N -body value for clusters on circular orbits (with $e = 0$ and in steady tidal fields) in the simulations; and our μ_{ev} is still within a factor of about three of the N -body rate for clusters on eccentric orbits with $e = 0.5$ in BM03 ($e \simeq 0.5$ – 0.6 is typical for tracers with an isotropic velocity distribution in a logarithmic potential; van den Bosch et al. 1999). This is very similar to the comparison of lifetimes in §3.1 for our original models based on $\mu_{ev} \propto \rho_h^{1/2}$. Moreover, our new estimate of μ_{ev} and that in BM03 are still subject to their own, separate uncertainties and reflect different idealizations and assumptions. For example, our rate still depends on the exact power-law exponent β at low masses in the initial GCMF, as discussed after equation (7); while the rate from BM03 still neglects gravitational shocks from disk crossings and passages by a discrete galactic bulge, and may additionally be biased low for $M_0 > 10^5 M_\odot$ if $x > 0.75$ at such masses. All of this—not to mention again the large uncertainties and possible systematics in the estimates of tidal radii needed to calculate Σ_t —makes the near agreement between equations (11) and (12) more striking than any apparent discrepancy.

In summary, although the relation $\mu_{ev} \propto \rho_h^{1/2} \simeq \text{constant}$ in time is rigorously correct only in rather specific circumstances, our GCMF models based on it in §2 are good proxies, in all respects, for models based on other plausible characterizations of relaxation-driven cluster mass loss. This result will likely be important for future studies of the mass functions of extragalactic cluster systems, where it may well be necessary to adopt procedures based on ρ_h rather than ρ_t or Σ_t because of the difficulty or impossibility of estimating tidal radii.

3.3. M_{TO} versus r_{gc} , and Velocity Anisotropy in GC Systems

In this paper we have directly modeled $dN/d \log M$ as a function only of GC density and age, and used the observed ρ_h (or ρ_t , or Σ_t) of clusters in relatively narrow ranges of Galactocentric position to show that such models are consistent with

the *current* near-constancy of the GCMF as a function of r_{gc} . Most other models in the literature for evaporation-dominated GCMF evolution, in either the Milky Way or other galaxies, instead predict the distribution explicitly as a function of r_{gc} at *any time*. They therefore need, in effect, to derive theoretical density–position relations for clusters in galaxies alongside their main GCMF calculations. This usually begins with the adoption of analytical potentials to describe the parent galaxies of GCs. Taking these to be spherical and static for a Hubble time allows the use of standard tidal-limitation formulae to write GC densities ab initio in terms of the (fixed) pericenters r_p of unique orbits in the adopted potentials. Cluster relaxation times and mass-loss rates μ_{ev} then follow as functions of r_p as well. Finally, specific initial mass, space, and velocity (or orbital eccentricity) distributions are chosen for entire GC systems, so that at all later times it is known what the dynamically evolved $dN/d \log M$ is for globulars with any single r_p ; how many clusters with a given r_p survive; and what the distributions of r_p and all dependent cluster properties are at any instantaneous position r_{gc} .

In this approach, if the GCMF began with a power-law rise towards low masses and its current peak is due entirely to cluster disruption, then a dependence of M_{TO} on r_p is expected in general, because the densities of tidally limited GCs decrease with increasing r_p . Thus, models along these lines that assume the orbit distribution of a GC system to be the same at all radii in a galaxy (i.e., that the time average of the ratio r_{gc}/r_p is independent of position) have typically had difficulty in accounting for the observed weak or non-correlation between M_{TO} and present r_{gc} in large galaxies. This is particularly a problem if it is assumed that the initial GCMF was a pure power law, with the same index at arbitrarily high masses as low (e.g., Baumgardt 1998; Vesperini 2001). It is potentially less of a concern if $dN/d \log M$ started as a Schechter function with an exponential cut-off at masses $M > M_c$, as we have assumed, since then the existence of a strict upper bound $M_{TO} \leq M_c$ (§2.2) means that the dependence of an evaporation-evolved M_{TO} on r_p and r_{gc} must saturate for small enough galactocentric radii (high enough GC densities). Even so, the “scale-free” models of FZ01, in which $M_c \simeq 10^6 M_\odot$ and all GCs in a Milky Way-like galaxy potential have the same time-averaged r_{gc}/r_p , still predict a gradient in M_{TO} versus r_{gc} that is stronger than observed.

FZ01 showed that, if they left all of their other assumptions unchanged, then a dependence of GCMF peak mass on r_{gc} could be effectively erased by an appropriately varying radial velocity anisotropy in the initial GC system. Thus, in their “Eddington” models the eccentricity of a typical cluster orbit increases with galactocentric distance (the time average of r_{gc}/r_p increases with radius), such that globulars spread over a larger range of current r_{gc} can have more similar r_p and associated M_{TO} . However, the initial velocity-anisotropy gradient required to fit the Milky Way GCMF data specifically is only marginally consistent with the observed kinematics of the GC system (e.g., Dinescu, Girard, & van Altena 1999).¹³ Subsequently, Vesperini et al. (2003) constructed broadly similar models for the GCMF of the Virgo elliptical M87 and concluded that there, too, a variable radial velocity anisotropy is required to match the observed M_{TO} versus r_{gc} ; but the model

anisotropy profile in this case is clearly inconsistent with the true velocity distribution of the GC system, which is observed to be isotropic out to large r_{gc} (Romanowsky & Kochanek 2001; Côté et al. 2001).

These results certainly suggest that some element is lacking in r_{gc} -oriented GCMF models developed as outlined above. But they do not mean that the fault lies with the main hypothesis, that the difference between the mass functions of young clusters and old GCs is due to the effects of slow, relaxation-driven disruption in the latter case. Any conclusions about velocity anisotropy depend on the totality of steps taken to connect the densities and positions of clusters; and it is possible that reasonable changes to one or more of these ancillary assumptions could make the models compatible with the observed kinematics of GCs in both the Milky Way and M87, without abandoning a basic physical picture of evaporation-dominated GCMF evolution that is otherwise quite successful.

One issue is that previous models have always specified evaporation rates a priori as functions of cluster density (or orbital pericenter), usually normalizing μ_{ev} so that $t_{dis}/t_{rh} \simeq 20$ –40 as in standard treatments of two-body relaxation. However, following our discussion in §3.1 and §3.2, it would seem worthwhile to investigate these models with μ_{ev} increased at fixed ρ_h or r_p to allow $t_{dis}/t_{rh} \approx 10$ (if $\beta \simeq 2$ for the low-mass power-law part of the initial GCMF) on average.

FZ01 and Vesperini et al. (2003) both consider velocity distributions parametrized by a galactocentric anisotropy radius, R_A , inside of which a cluster system is essentially isotropic and beyond which it is increasingly dominated by radial orbits. In these terms, the difficulty with the published models is that, to reproduce the observed insensitivity of M_{TO} to r_{gc} given standard normalizations of μ_{ev} , they require values of R_A that are smaller than allowed by observations (especially for M87). Increasing R_A to more realistic values while keeping the normalization of μ_{ev} fixed leads to a stronger gradient in M_{TO} : the orbits of GCs at small $r_{gc} \lesssim R_A$ remain closely isotropic and the typical r_p and M_{TO} are essentially unchanged, while at large galactocentric distances the cluster orbits are on average less radial than before, with larger r_p , lower densities, and lower evolved M_{TO} for a given r_{gc} . This effect is illustrated, for example, in Figure 9 of FZ01. However, it can be compensated at least in part by increasing μ_{ev} by a common factor for all GCs, with the new, larger R_A fixed, *if the initial mass function is assumed to have been a Schechter function rather than a pure power law extending to arbitrarily high masses*. A faster evaporation rate will then lead to a (roughly) proportionate increase in the evolved GCMF peak mass for GCs with relatively low densities, i.e., those at large r_{gc} and r_p ; but the increase in M_{TO} will be *smaller*, and eventually even negligible, for higher-density clusters at progressively smaller r_{gc} —again because M_{TO} grows less than linearly with $\mu_{ev} \propto \rho_h^{1/2}$ when there is an upper limit $M_{TO} < M_c$ due to an exponential cut-off in the initial $dN/d \log M_0$. Thus, the qualitative effect of increasing the normalization of μ_{ev} in models with radially varying GC velocity anisotropy is to weaken the amount of radial-orbit bias required to fit an observed M_{TO} versus r_{gc} .

Another point, emphasized by FZ01, has to do with the standard starting assumption that GCs orbit in galaxies that are perfectly static and spherical. In reality, large galaxies grow hierarchically. In this case, even if the normalization of μ_{ev} is not changed, much of the burden for the weaken-

¹³ The fact that clusters on radial orbits are preferentially disrupted lessens any inconsistency between the radial anisotropy required in the initial velocity distribution and observational constraints on the present velocity distribution.

ing or erasing of any initial gradients in M_{TO} versus r_{gc} may be transferred from velocity anisotropy to the time-dependent evolution of the galaxies themselves. Violent relaxation, major mergers, and smaller accretion events all work to move clusters between different parts of galaxies and between different progenitors, scrambling and combining any number of pericenter–density– M_{TO} relations. Any position dependences in the GC ρ_h distribution and in M_{TO} itself for the final galaxy are therefore bound to be weaker, more scattered, and more difficult to relate accurately to a cluster velocity distribution than in the case of a monolithic, non-evolving potential. Allowing for a non-spherical galaxy potential would have qualitatively the same effect, because in this case any cluster explores a range of pericenters and different maximum tidal fields on each of its orbits.

In this situation, it may be important to ask how evaporation rates can still be approximately constant in time—so that cluster masses still decrease approximately linearly with t as our models assume—if the tidal field around any given GC changes significantly over time. Thus, consider first a system of GCs in a single, static galaxy potential. The mass-evolution curve for each cluster is approximately a straight line, $M(t) \simeq M_0 - \mu_{\text{ev}} t$, with μ_{ev} depending on some measure of internal density, which may be $\rho_h^{1/2}$, $\rho_t^{1/2}$, or $\Sigma_t^{3/4}$. The average mass-evolution curve for the entire system of clusters is also approximately linear, $\langle M(t) \rangle \simeq \langle M_0 \rangle - \langle \mu_{\text{ev}} \rangle t$. If now a merger or other event rearranges the clusters in the galaxy, then after the event the mass-loss rates of some clusters will be higher than before and the rates of other clusters will be lower than before. However, if the mean density of the galaxy as a whole is roughly the same after the event as before, then so too will be the average of the GC densities, because of tidal limitation. The average $\langle \mu_{\text{ev}} \rangle \propto \langle \rho_h^{1/2} \rangle$ (say) will differ still less between the pre- and post-merger systems. Thus, although using instantaneous densities to estimate the past μ_{ev} of individual clusters may err on the high side for some clusters and on the low side for others, these errors will average away to a small or even zero net bias. The approximation $\mu_{\text{ev}} \simeq \text{constant}$ in time in our GCMF models will then still be valid in the mean, and the average $\langle M(t) \rangle$ dependence of sufficiently large numbers of clusters will remain roughly linear.

This type of scenario might be expected to pertain at least to galaxies that evolve on the fundamental plane, since this entails a connection between the total (baryonic plus dark) masses and circular speeds of galaxies, of the form $M_{\text{gal}} \propto V_c^3$ or $M_{\text{gal}} \propto V_c^4$. By the virial theorem, the average densities scale as $\rho_{\text{gal}} \propto V_c^6/M^2$, and thus $\rho_{\text{gal}} \propto M_{\text{gal}}^0$ or $\rho_{\text{gal}} \propto M_{\text{gal}}^{-1/2}$. Insofar as $\langle \rho_h \rangle \propto \langle \rho_t \rangle \propto \rho_{\text{gal}}$ for the GCs, the system-wide average $\langle \mu_{\text{ev}} \rangle \propto \langle \rho_h^{1/2} \rangle$ should therefore not change drastically even after a major merger between two fundamental-plane galaxies; at most, the ratio of final to initial $\langle \mu_{\text{ev}} \rangle$ will be roughly of order the $-1/4$ power of the ratio of final to initial M_{gal} . Note that this line of reasoning is closely related to that applied by FZ01 to explain the small observed galaxy-to-galaxy differences in the average turnover masses of entire GC systems (although non-zero differences do exist, and can be accommodated in these sorts of arguments; see Jordán et al. 2006, 2007).

A full exploration of questions such as these about the wide range of ingredients in current GC-plus-galaxy models will most likely require large N -body simulations set in a realistic, cold dark matter cosmology. Until these can be carried out,

it is our view that the kinematics of globular cluster systems cannot be used as decisive side constraints on theories for the GCMF.

4. CONCLUSIONS

We have shown that the mass function $dN/d \log M$ of globular clusters in the Milky Way depends significantly on cluster half-mass density, ρ_h , with the peak or turnover mass M_{TO} increasing and the width of the distribution decreasing as ρ_h increases. This behavior is expected if the GCMF initially rose towards masses below the present turnover scale—as the mass functions of young cluster systems like that in the Antennae galaxies do—and has evolved to its current shape via the slow depletion of low-mass clusters over Gyr timescales, primarily through relaxation-driven evaporation. The fact that M_{TO} increases with cluster density favors evaporation over external gravitational shocks as the primary mechanism of low-mass cluster disruption, since the mass-loss rates associated with shocks depend inversely on cluster density. Our results therefore add to previous arguments supporting an interpretation of the GCMF in terms of evaporation-dominated evolution, based on the fact that $dN/d \log M$ scales as $M^{1-\beta}$ with $\beta \simeq 0$ in the low-mass limit (Fall & Zhang 2001).

The observed GCMF as a function of ρ_h is fitted well by simple models in which the initial distribution was a Schechter function, $dN/d \log M_0 \propto M_0^{1-\beta} \exp(-M_0/M_c)$ with $\beta = 2$ and $M_c \simeq 10^6 M_\odot$ assumed, and in which clusters have been losing mass for a Hubble time at roughly steady rates that can be estimated from their current half-mass densities as $\mu_{\text{ev}} \propto \rho_h^{1/2}$. We have shown that, although this prescription is approximate, it captures the main physical dependence of relaxation-driven evaporation. In particular, it leads to model GCMFs that are entirely consistent with those resulting from alternative characterizations of evaporation rates in terms of cluster tidal densities ρ_t or mean surface densities Σ_t (§3.2). The normalization of μ_{ev} at a given ρ_h (or ρ_t , or Σ_t) required to fit the GCMF implies total cluster lifetimes that are within range of the lifetimes typically obtained in theoretical studies of two-body relaxation, although our values may be slightly shorter than the theoretical ones if the low-mass, power-law part of the initial cluster mass function was as steep as we have assumed.

Taking clusters in various bins of central concentration c and Galactocentric radius r_{gc} and using their (individual) observed densities as direct input to our models yields dynamically evolved GCMFs as functions of c and r_{gc} that agree well with all data. This again indicates that the most fundamental physical dependence in the GCMF is that on cluster density. Moreover, our models for $dN/d \log M$ versus r_{gc} obtained in this way are consistent in particular with the well-known insensitivity of the GCMF peak mass to Galactocentric position. This is seen to follow from a significant variation of M_{TO} with ρ_h (or ρ_t , or Σ_t)—due in our analysis to evaporation-dominated cluster disruption—combined with substantial scatter in the GC densities at any Galactocentric position.

We have not invoked an anisotropic GC velocity distribution to explain the observed weak variation of M_{TO} with r_{gc} ; indeed, we have made no predictions or assumptions whatsoever about velocity anisotropy. We have emphasized that, when velocity anisotropy enters other long-term dynamical-evolution models for the GCMF, it is only in conjunction with several additional, interrelated assumptions made as part of

larger efforts to derive theoretical density- r_{gc} relations for GCs—which we have not attempted to do here. The apparent need in some current models for a strong bias towards high-eccentricity cluster orbits to explain the near-constancy of M_{TO} versus r_{gc} might well be avoided by changing one or more ancillary assumptions in the models, without having to discard the underlying idea that the peak and low-mass shape of the GCMF are the result of relaxation-driven cluster disruption.

It clearly will be of interest to test and refine the main ideas in this paper through modeling of the GCMFs in other galaxies. For the time being at least, doing so will require the estimation of approximate mass-loss rates using cluster half-mass densities rather than tidal quantities, simply because GC half-light radii can be measured accurately in many systems beyond the Local Group, whereas tidal radii are much more

model-dependent and difficult to observe. Chandar, Fall, & McLaughlin (2007) have recently shown that the peak mass of the GCMF in the Sombrero galaxy (M104) increases with ρ_h in a way that is reasonably well described by sums of evolved Schechter (1976) functions as in the models presented in this paper. It should be relatively straightforward to pursue similar studies in other nearby galaxies.

We thank Michele Trenti, Douglas Heggie, Bill Harris, Rupali Chandar, and Bruce Elmegreen for useful discussions and comments. SMF acknowledges support from the Ambrose Monell Foundation and from NASA grant AR-09539.1-A, awarded by the Space Telescope Science Institute, which is operated by AURA, Inc., under NASA contract NAS5-26555.

REFERENCES

- Aguilar, L., Hut, P., & Ostriker, J. P. 1988, *ApJ*, 335, 720
 Barmby, P., Huchra, J. P., & Brodie, J. P. 2001, *AJ*, 121, 1482
 Barmby, P., McLaughlin, D. E., Harris, W. E., Harris, G. L. H., & Forbes, D. A. 2007, *AJ*, 133, 2764
 Baumgardt, H. 1998, *A&A*, 330, 480
 Baumgardt, H. 2001, *MNRAS*, 325, 1323
 Baumgardt, H., & Makino, J. 2003, *MNRAS*, 340, 227 (BM03)
 Binney, J., & Tremaine, S. 1987, *Galactic Dynamics* (Princeton: Princeton University Press)
 Burkert, A., & Smith, G. H. 2000, *ApJ*, 542, L95
 Caputo, F., & Castellani, V. 1984, *MNRAS*, 207, 185
 Chandar, R., Fall, S. M., & McLaughlin, D. E. 2007, *ApJ*, 668, L119
 Chandrasekhar, S. 1942, *Principles of Stellar Dynamics* (Chicago: University of Chicago Press)
 Chernoff, D. F., & Weinberg, M. D. 1990, *ApJ*, 351, 121
 Côté, P., et al. 2001, *ApJ*, 559, 828
 Dinescu, D. I., Girard, T. M., & van Altena, W. F. 1999, *AJ*, 117, 1792
 Djorgovski, S., & Meylan, G. 1994, *AJ*, 108, 1292
 Elmegreen, B. G., & Efremov, Y. N. 1997, *ApJ*, 480, 235
 Fall, S. M., & Rees, M. J. 1977, *MNRAS*, 181, 37P
 Fall, S. M., & Zhang, Q. 2001, *ApJ*, 561, 751 (FZ01)
 Fukushima, T., & Heggie, D. C. 2000, *MNRAS*, 318, 753
 Giersz, M. 2001, *MNRAS*, 324, 218
 Giersz, M., & Heggie, D. C. 1996, *MNRAS*, 279, 1037
 Gnedin, O. Y. 1997, *ApJ*, 487, 663
 Gnedin, O. Y., & Ostriker, J. P. 1997, *ApJ*, 474, 223
 Gnedin, O. Y., Lee, H. M., & Ostriker, J. P. 1999, *ApJ*, 522, 935
 Harris, W. E. 1996, *AJ*, 112, 1487
 Harris, W. E. 2001, in *Star Clusters* (28th Saas-Fee Advanced Course) ed. L. Labhardt & B. Binggeli (Berlin: Springer), 223
 Harris, W. E., & Pudritz, R. E. 1994, *ApJ*, 429, 177
 Harris, W. E., Harris, G. L. H., & McLaughlin, D. E. 1998, *AJ*, 115, 1801
 Heggie, D. C., Giersz, M., Spurzem, R., and Takahashi, K. 1998, *HiA*, 11, 591
 Hénon, M. 1961, *Ann. d'Astrophys.*, 24, 369
 Innanen, K. A., Harris, W. E., & Webbink, R. F. 1983, *AJ*, 88, 338
 Johnstone, D. 1993, *AJ*, 105, 155
 Joshi, K. J., Nave, C. P., & Rasio, F. A. 2001, *ApJ*, 550, 691
 Jordán, A., et al. 2005, *ApJ*, 634, 1002
 Jordán, A., et al. 2006, *ApJ*, 651, L25
 Jordán, A., et al. 2007, *ApJS*, 171, 101
 Kavelaars, J. J., & Hanes, D. A. 1997, *MNRAS*, 285, L31
 Lee, H. M., & Goodman, J. 1995, *ApJ*, 443, 109
 King, I. R. 1958, *AJ*, 63, 109
 King, I. R. 1959, *AJ*, 64, 351
 King, I. R. 1966, *AJ*, 71, 276
 Lee, H. M., & Ostriker, J. P. 1987, *ApJ*, 322, 123
 McLaughlin, D. E. 2000, *ApJ*, 539, 618
 McLaughlin, D. E., & van der Marel, R. P. 2005, *ApJS*, 161, 304
 Murali, C., & Weinberg, M. D. 1997, *MNRAS*, 291, 717
 Okazaki, T., & Tosa, M. 1995, *MNRAS*, 274, 48
 Ostriker, J. P., & Gnedin, O. Y. 1997, *ApJ*, 487, 667
 Parmentier, G., & Gilmore, G. 2007, *MNRAS*, 377, 352
 Prieto, J. L., & Gnedin, O. Y. 2006, preprint (astro-ph/0608069)
 Romanowsky, A. J., & Kochanek, C. S. 2001, *ApJ*, 553, 722
 Schechter, P. 1976, *ApJ*, 203, 297
 Smith, G. H., & Burkert, A. 2002, *ApJ*, 578, L51
 Spitler, L., Larsen, S. S., Strader, J., Brodie, J. P., Forbes, D. A., & Beasley, M. A. 2006, *AJ*, 132, 1593
 Spitzer, L. 1987, *Dynamical Evolution of Globular Clusters* (Princeton: Princeton Univ. Press)
 Takahashi, K., & Portegies Zwart, S. F. 1998, *ApJ*, 503, L49
 Takahashi, K., & Portegies Zwart, S. F. 2000, *ApJ*, 535, 759
 Trenti, M., Heggie, D. C., & Hut, P. 2007, *MNRAS*, 374, 344
 van den Bosch, F. C., Lewis, G. F., Lake, G., & Stadel, J. 1999, *ApJ*, 515, 50
 Vesperini, E. 1997, *MNRAS*, 287, 915
 Vesperini, E. 1998, *MNRAS*, 299, 1019
 Vesperini, E. 2000, *MNRAS*, 318, 841
 Vesperini, E. 2001, *MNRAS*, 322, 247
 Vesperini, E., & Heggie, D. C. 1997, *MNRAS*, 289, 898
 Vesperini, E., & Zepf, S. E. 2003, *ApJ*, 587, L97
 Vesperini, E., Zepf, S. E., Kundu, A., & Ashman, K. M. 2003, *ApJ*, 593, 760
 Waters, C. Z., Zepf, S. E., Lauer, T. R., Baltz, E. A., & Silk, J. 2006, *ApJ*, 650, 885
 Zhang, Q., & Fall, S. M. 1999, *ApJ*, 527, L81